

# **Model Membrane Studies Related To Ionic Transport In Biological Systems**

By S. S. Nelson and I. Blei, Melpar, Incorporated, for Office of Saline Water, J. A. Hunter, Acting Director; W. Sherman Gillam, Assistant Director, Research; H. E. Podall, Chief, Biosciences Division

UNITED STATES DEPARTMENT OF THE INTERIOR • Stewart L. Udall, Secretary  
Frank C. Di Luzio, Assistant Secretary for Water Pollution Control

Created in 1849, the Department of the Interior-- America's Department of Natural Resources--is concerned with the management, conservation, and development of the Nation's water, wildlife, mineral, forest, and park and recreational resources. It also has major responsibilities for Indian and Territorial affairs.

As the Nation's principal conservation agency, the Department of the Interior works to assure that nonrenewable resources are developed and used wisely, that park and recreational resources are conserved for the future, and that renewable resources make their full contribution to the progress, prosperity, and security of the United States--now and in the future.

#### FOREWORD

This is the two hundred and twenty-first of a series of reports designed to present accounts of progress in saline water conversion with the expectation that the exchange of such data will contribute to the long-range development of economical processes applicable to large-scale, low-cost demineralization of sea or other saline water.

Except for minor editing, the data herein are as contained in the reports submitted by Melpar, Incorporated, under Contract No. 14-01-0001-387, covering research carried out through July 1966. The data and conclusions given in the report are essentially those of the contractor and are not necessarily endorsed by the Department of the Interior.

## TABLE OF CONTENTS

	<u>Page</u>
1. INTRODUCTION	1
2. EXPERIMENTAL PROGRAMS	2
2.1 Multilayer Crystals	2
2.1.1 Langmuir-Blodgett Technique	2
2.1.2 Construction Details	3
2.1.3 Film Building Procedures	11
2.1.4 Force Area Determinations	12
2.1.5 Deposition of Barium Stearate	13
2.1.6 Multilayer Concentration Cell	14
2.1.7 Cell Characteristics	15
2.1.8 General Protocol for Langmuir- Blodgett Membrane Manufacture	15
2.2 Cost Membranes	21
2.2.1 Preliminary Remarks	21
2.2.2 Preparation of Potassium Oleate-Collodion Membranes	22
2.2.3 Preparation of Collodion- Polysoap Membranes	22
2.2.4 Determination of Membrane Properties	23
3. RESULTS	25
3.1 Langmuir-Blodgett Techniques	25

TABLE OF CONTENTS  
(cont'd.)

	<u>Page</u>
3.1.1 Effect of Orientation on Selectivity	25
3.1.2 Multilayer Structure Formation of New Materials	26
3.1.3 Formation of Barium Stearate Structures and Effects of Pressure	33
3.1.4 Effect of Dipping Rate	33
3.1.5 Effect of Copper Ion	34
3.1.6 Effect of pH	35
3.1.7 Barium Stearate Multilayer	35
3.1.8 Barium Stearate Multilayer - Effects of Irradiation	41
3.1.9 Adhesion to Glass	41
3.1.10 Adhesion to "Millipore" Filter Material	41
3.1.11 Membrane Characteristics	42
3.2 Soap and Polysoap Membranes	51
3.2.1 Collodion - Potassium Oleate Membranes	51
3.2.2 Matrix-Free Soap Systems	62

TABLE OF CONTENTS  
(cont'd)

	<u>Page</u>
4. DISCUSSION	72
4.1 Multilayer Crystals	72
4.2 Soap and Polysoap Membranes	74
4.2.1 Polysoaps	74
4.2.2 Transport Numbers	75
4.2.3 Junction Potentials	75
4.2.4 Nature of the Reversible Transition	76
4.2.5 Permselectivity "Pore" Size, Anesthesization and Other Considerations	76
5. CONCLUSIONS AND SUMMARY	85
6. RECOMMENDATIONS FOR FUTURE WORK	87
7. REFERENCES	88

## LIST OF ILLUSTRATIONS

<u>Figure</u>		<u>Page</u>
1	Diagram of Surface Balance	4
2	Circuit Diagram of Photocell Amplifier	6
3	Block Diagram of Film Compression Servomechanism	7
4	Block Diagram of Langmuir-Blodgett Dipping Servomechanism	8
5	Diagram of Still	9
6	Concentration Cell	16
7	Force-Area Curves of Cerotic Acid on pH 1.3 Substrate	27
8	Force-Area Curves of Lecithin and Cephalin Films on Barium-Containing Substrate	30
9	Force-Area Curves of Stearic Acid and Stearyl Phosphoric Acid	31
10	Force-Area Curves of Calcium Stearyl Phosphate and Calcium Lecithinate	32
11	Recrystallization Changes on X-ray Diffraction Peak from 49.3Å Crystal Spacing of Barium Stearate Multilayer at 70°C	36
12	Long Spacing of X-rays from Polycrystalline Barium Stearate Cu K $\alpha$ Radiation	37
13	Long Spacing Reflections of X-rays From Barium Stearate Multilayer	39

LIST OF ILLUSTRATIONS  
(cont'd.)

<u>Figure</u>		<u>Page</u>
14	X-ray Diffraction Curves of Principle Peak ( $1.75^\circ = 49.3\text{\AA}$ ) of Barium Stearate Multilayer Heated to Several Temperatures	40
15	Barium Stearate X-ray Diffraction Intensity vs Temperature	43
16	Conductance of Barium Stearate Multilayer Membranes vs Temperature	47
17	X-ray Diffraction Intensity vs pH	48
18	Conductivity of pH 5.5 Barium Stearate Multilayer Membranes vs Temperature and Frequency	49
19	Dielectric Constant and Loss Factor of Barium Stearate Multilayer vs Temperature	49a
20	NMR Spectra of Wet, Hydrated, and Dehydrated Barium Stearate Powder, "Wet" Sample Dried one Hour Over Silica Gel at 1 mm Pressure to Remove Unbound Water	52
21	The Effect of Temperature on Membrane Bi-ionic Potential	54
22	Electrolyte Diffusion Through a Collodion-Potassium Oleate Membrane	56
23	The Effect of Temperature on Membrane Bi-ionic Potential	57
24	The Effect of Temperature on Membrane Bi-ionic Potential	58

LIST OF ILLUSTRATIONS  
(Cont'd.)

<u>Figure</u>		<u>Page</u>
25	Bi-ionic Potential of 0.1 M Sodium Stearate Gel as a Function of Electrolyte Concentration	63
26	Temperature Dependence of BIP and Check of Pauling Hypothesis	81
27	Temperature Dependence of BIP and Test of Reversibility of the Effect of $\text{CH}_3\text{Cl}$	82
28	BIP vs Concentration of $\text{CH}_3\text{Cl}$ (PS 3-1-1-1 Membrane; 1 M NaCl/KCl Couple, $T = 1.4^\circ\text{C}$ )	83

## LIST OF TABLES

<u>Table</u>		<u>Page</u>
1	Description of Barium Stearate Manufacture and Fate	45
2	Determinations of the Dielectric Constant of Hydrated Barium Stearate Multilayers	50
3	Collodion-Potassium Oleate Membrane Potentials	53
4	Concentration Cell Potentials	59
5	Tabulated Bi-Ionic Potentials (1M)	61
6	Tabulated Bi-Ionic Potentials (0.5M)	61
7	Collodion-Polysoap Membrane (3-3-3) Potentials	64
8	Collodion-Polysoap Membrane (2-2-2) Potentials	64
9	Diffusion Rates and BIP (Bi-Ionic Potential) Values of Non-Selective Collodion as a Function of Membrane Thickness	65
10	Collodion Diffusion Rates and BIP's as a Function of Ether-Acetone Ratio	65
11	Effect of Thickness on Diffusion Through Glycerol Graded Collodion	66
12	Permselective Characteristics (Trans- port Numbers) of the Collodion Used in The Preparation of PS 3-1-1-1 and PS 3-1-2-1 Membranes	66

LIST OF TABLES  
(Cont'd.)

<u>Table</u>		<u>Page</u>
13	Permselective Properties of a PS 3-1-1-1 Membrane Immediately After Casting and Air Drying	67
14	Permselective Properties of a PS 3-1-1-1 Membrane After Air Drying for 24 Hours	67
15	Permselective Properties of a PS 3-1-1-1 Membrane After Air Drying For One Week	68
16	Membrane Transport Numbers for Various (non-polymeric) Oleate Systems	69
17	Membrane Transport Numbers; PS 3-4-4-4 Membrane	69
18	Anion Permselectivity of a PS 3-1-2-1 Membrane and Calculated BIP's	70
19	Cation Permselectivity (various anions) of PS 3-1-2-1 Membrane and Calculated BIP's	70
20	Further Tests of the Pauling Theory of Molecular Anesthesia - Effect of Argon and Nitrogen Saturation (one atmosphere) on BIP	71

## 1. INTRODUCTION

The research performed under this contract was directed toward determining the influence of lipid phase transitions on the diffusion characteristics of sodium and potassium in the polar regions of condensed polar lipid-like systems, and the bearing of these effects on ionic regulatory mechanisms of biological membranes. During the first phase of these studies systems resembling crystals of cephalin, lecithin and other appropriate lipids were prepared. Bi-ionic potentials and self-diffusion coefficients of barium along the crystal axis and polar sheets were determined. Electrical and diffusion parameters were also measured following modification of the crystal by heat treatment. The data obtained in this manner were used to test the validity of the hypothesis that the discrimination of sodium from potassium in crystalline solids containing oxygen atoms is at the root of the biological differentiation of these atoms; and that sodium is differentiated from potassium and prevented from entering the resting cell through order-disorder transitions in the ionic or polar portions of the cell membrane.

It was thought that a similarity may exist between soaps and naturally occurring lipids. The commonly held property was thought to be the existence of a critical temperature, similar to the Kraft point, above which the micelles are liquid in nature and below which they undergo a transition to the crystalline state.

Owing to the extremely high impedance of the various multilayer lipid-like systems, and other experimental difficulties, it was difficult to observe truly reversible and reproducible temperature transitions. In order to bolster these tentative findings it was decided to study temperature transitions in other micelle-forming, oxygen containing systems. The problem of high impedance was resolved by resorting to large cast membranes of laminar construction. Various alkali halide concentration and bi-ionic cell systems were studied with respect to the parameters of temperature, electrochemical potential and diffusion rates. A low temperature transition was observed (in bi-ionic systems)

which was partially reversible with respect to "anesthetization" by nonpolar agents (eg. chloroform). The later finding was consistent with the predictions of the Pauling "Theory of Molecular Anesthesia."<sup>1</sup>

## 2. EXPERIMENTAL PROGRAMS

### 2.1 Multilayer Crystals

#### 2.1.1 Langmuir-Blodgett Technique

This technique was used to produce "crystals" by the successive deposition of mono-molecular layers of ionic lipid spread at the air-water interface onto the surface of quartz slides. A film of fatty acid or soap was formed on the surface of water in a trough; the surface pressure determined, and the film transferred to a glass or metal slide by dipping the slide slowly through the film, maintaining the surface pressure constant. As the slide is drawn out of the trough through the water the film is deposited with the non-polar side toward the surface of the slide. Thus symmetrical heads tend to be deposited. A layer of polar "heads" is separated from the next similar layer by a double layer of hydrocarbon "tails".

To successfully deposit monolayers on solids, a monolayer in the liquid-condensed, or solid state, is required. This was considered necessary, because it is only in the condensed state that the molecules making up a monolayer will be highly oriented and resemble a two dimensional crystal. Lateral interaction is also high enough to lend cohesiveness to the film for reproducible deposition. The surface pressure of the film must remain constant during deposition if the surface density of the film being deposited is to be identical to that of the film on the water. A knowledge of the solid state characteristics of the deposited film depends on a thorough knowledge of the structure of the monolayer at the air-water interface. The two critical parameters here are the surface density (the area per molecule) and the orientation of each molecule which may be estimated by the surface dipole moment determined through measurements of the surface potential.

In order to study the mobility of the various cations in the synthetic crystals, salts of the ionic lipids were deposited. This was accomplished by spreading the lipids on a solution containing the cations required. Salt formation occurred under these conditions, thereby producing the desired surface species. It is necessary to thoroughly characterize each of these ionic lipid salts so that the surface state appropriate for deposition may be obtained. Before any solid state measurements can be made, precise surface chemical studies had to be done.

### 2.1.2 Construction Details

The following is a description of the apparatus used for the preparation of multilayer membranes by the Langmuir-Blodgett technique. A quartz trough, approximately 25 cm wide X 75 cm long X 2 cm deep was modified by fusing to it, a quartz well about 5.5 cm long X 8.5 cm wide X 9 cm deep about 9 cm from one end. The trough is supported by a frame of lucite and stainless steel and is equipped with leveling screws. The entire assembly is enclosed in a lucite windowed cabinet with all operating controls external. (Figure 1)

A "Cenco Hydrophil Torsion Balance" is mounted on the frame supporting the trough. This balance contains a torsion wire, a vernier scale capable of being read to  $0.1^\circ$  of rotation, a worm gear drive with shaft extended outside the cabinet, and a zero adjustment. Attached to the center of the torsion wire are two nickle arms extending down to below the top of the trough. These arms pass through guide holes in a movable mica strip, coated with paraffin to float in the trough, which is the surface-pressure sensing element. Attached to the top of the torsion wire is an aluminum vane, which interrupts a light path to a photocell assembly, mounted on the top of the cabinet, when the torsion-wire assembly is in balance.

The trough and well are filled with distilled water. Floating in the trough is a paraffin-coated mica frame which encloses a surface area of 1441 cm. The mica frame is constrained in the trough by silk threads at each corner. The

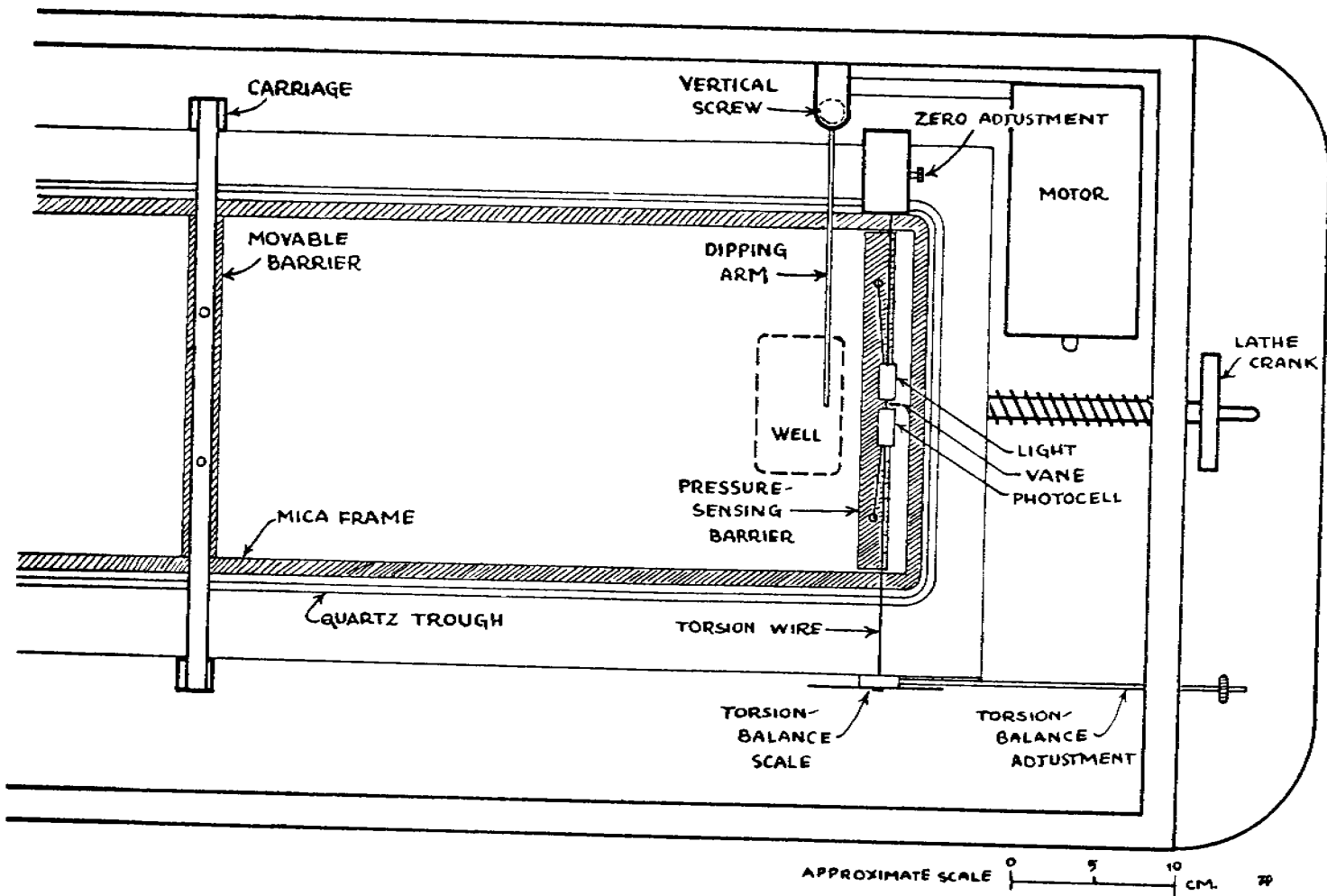


Figure 1. Diagram of Surface Balance

surface-pressure sensing mica barrier is loosely attached to the mica frame by vaseline-coated silk threads attached to each side, floating on the surface of the water. The threads are loose enough so that the barrier is free to move without resistance over a working range of 1-2 cm. The surface film is constrained by the barrier and threads from reaching the water behind the barrier.

A second barrier of paraffin-coated mica floats in the trough in contact with the mica frame and is held in position by a movable carriage with stainless steel pins extending through guide holes in the barrier. The carriage is mounted on a lathe bed and driven by either a hand crank or by a variable-speed motor. The motor may be disengaged by a magnetic clutch which eliminates vibration.

Automatic control of film pressure is provided as follows. The output of the photocell, in turn controls the film-compressing drive motor. (Figures 2 and 3) When the surface pressure is less than the setting of the torsion balance, the drive motor operates to advance the movable barrier and compress the film. When the pressure is sufficient to push the torsion-balance vane back into the light path, the motor is stopped. Thus, as surface film is removed to form a deposited membrane the surface area will be reduced, maintaining constant film pressure.

A device has been constructed for dipping slides through a gear-reduction box to a vertical screw. A sleeve rides on the screw and on vertical guides; a lateral arm extends over the dipping well in the trough. Adjustable clips hold microscope slides or metal plates in position for dipping. (Figure 4)

A two-stage quartz still with ion-exchange water inlet filter with a capacity of 1.5 liters per hour was used to supply distilled water. Figure 5 is a schematic diagram of this still. The ion-exchange column contains about 4 kg of "Lewatit KSN" resin in the sodium form; the column is contained in a plastic tube 10 cm wide and 60 cm long. Water passing through the column flows into the first-stage boiler. Steam condensed on the inner surface

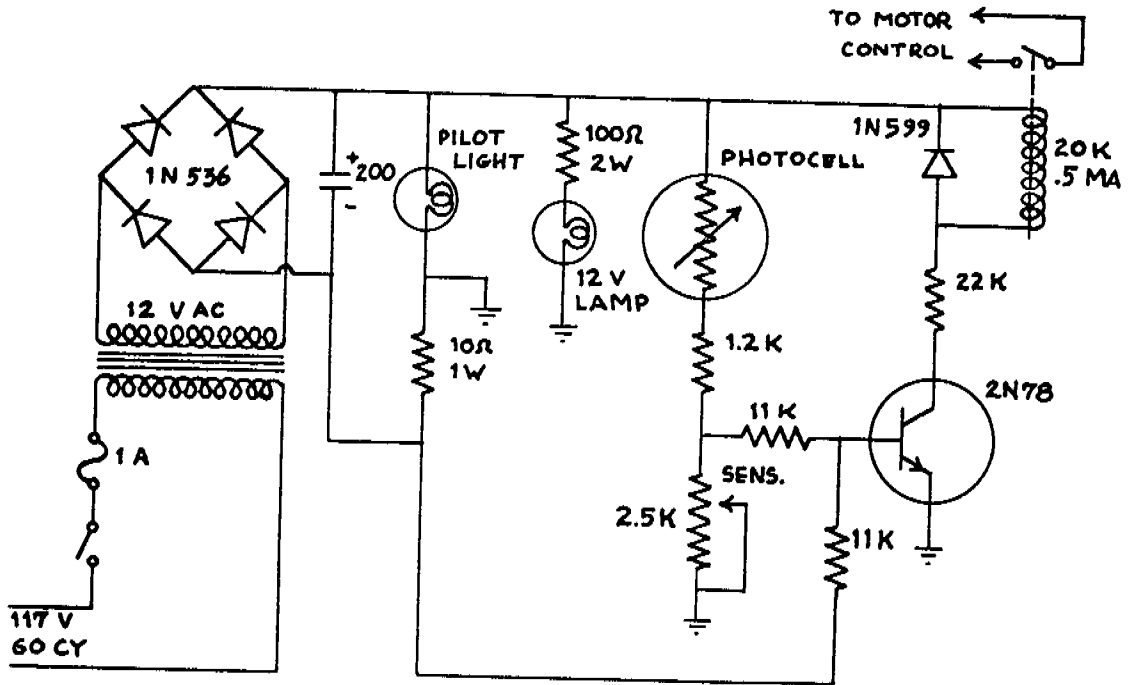


Figure 2. Circuit Diagram of Photocell Amplifier

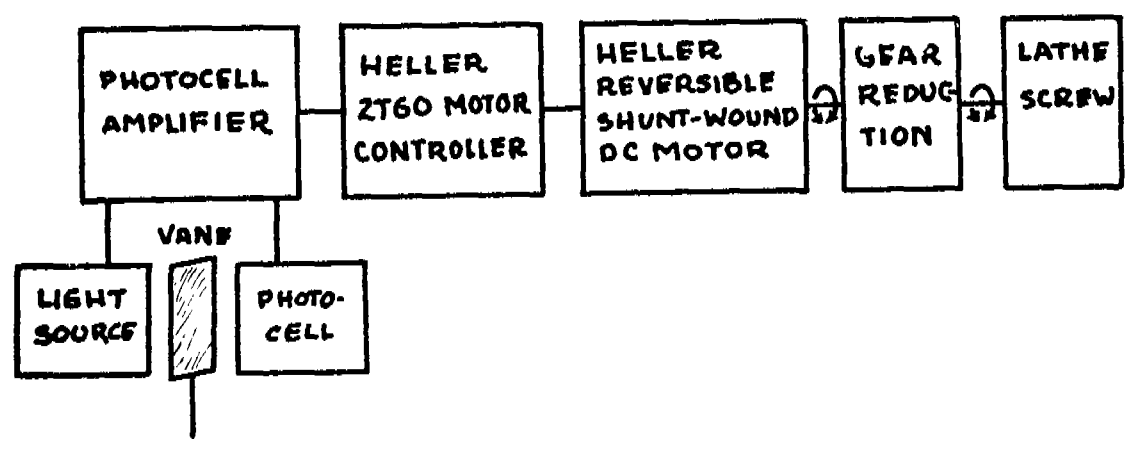


Figure 3. Block Diagram of Film Compression Servomechanism

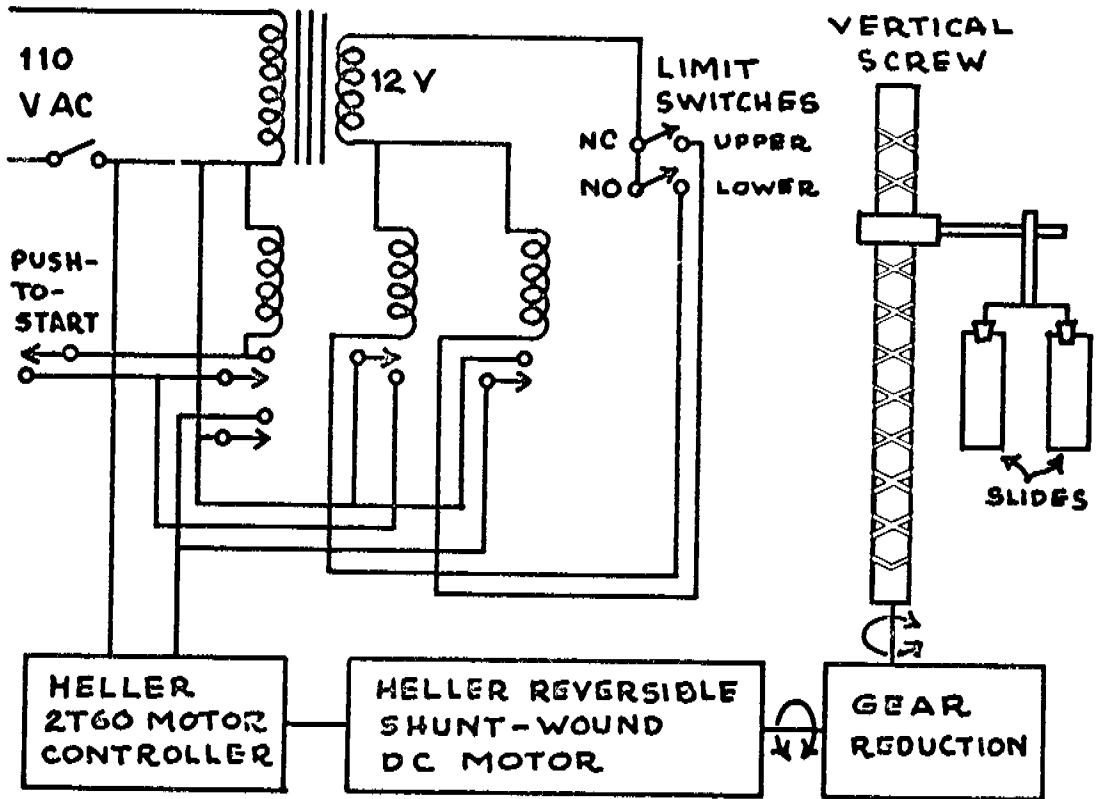


Figure 4. Block Diagram of Langmuir - Blodgett Dipping Servomechanism

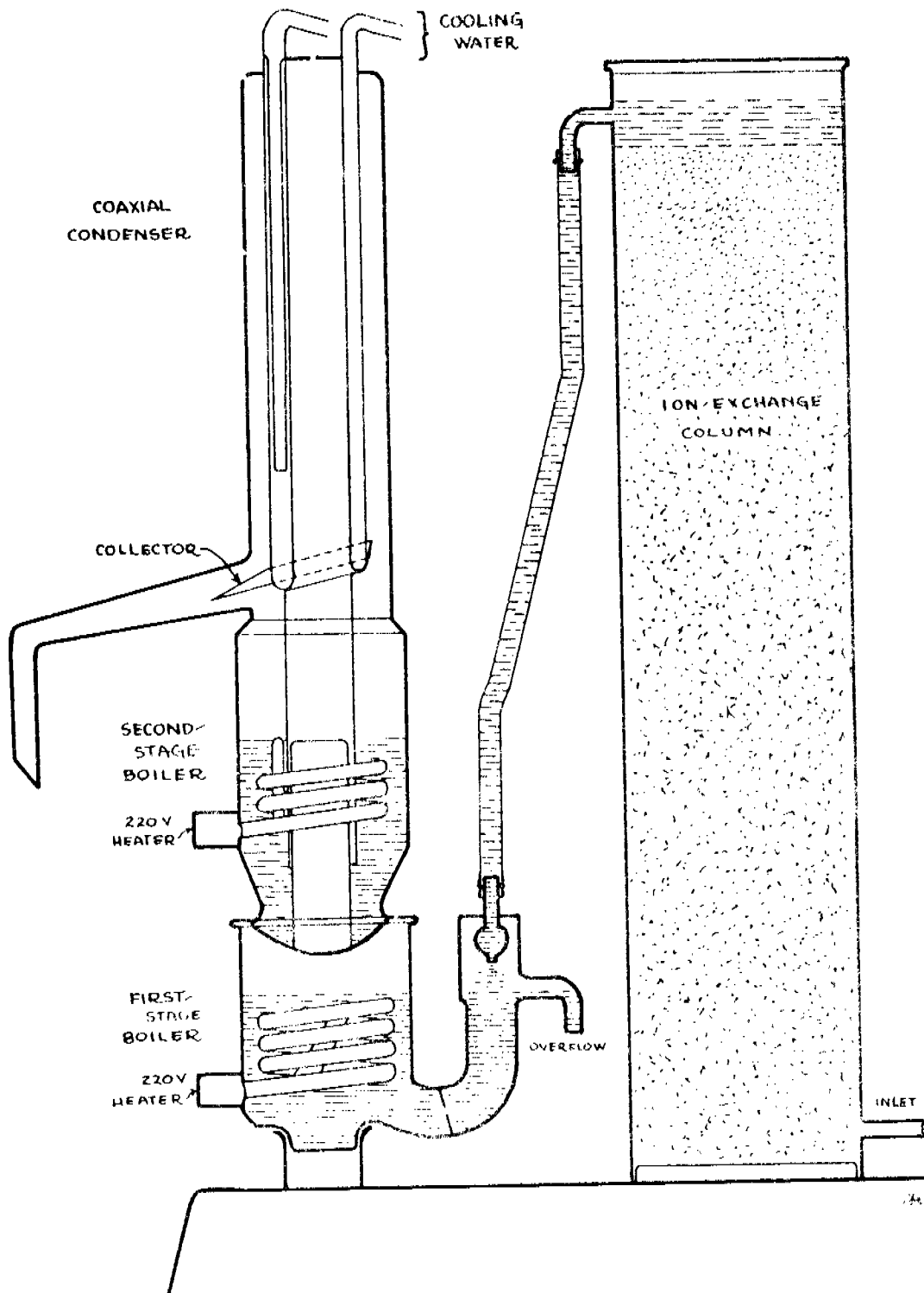


Figure 5. Diagram of Still

of a coaxial double condenser, and the distillate flows into the second-stage boiler. Steam from the second-stage condenses on the outer surface of the condenser, and the distillate flows out through a side arm to a receiving flask. Both boilers, the condenser, and the receiving flask are of transparent quartz. The resulting distilled water is reliably free of sodium and potassium.

Several grams of stearic acid were prepared for use as a reference standard and in experiments on films of stearic acid and stearate soaps. This material had been purified by three crystallizations, and three zone refinements.

Calibration of the torsion balance indicates that measurements are reproducible to within  $.01^\circ$  of rotation of the torsion wire. The sensitivity of the balance was found to be 1.615 dynes per degree. Thus, for a surface-pressure-sensing barrier 20 cm long the limit of detection was about 0.01 dynes per cm. With the trough filled and a film in compression, viscosity effects damp out oscillations with the net result that the surface pressure may be held to about 0.1 dynes per cm by the servomechanism during deposition of the film on a slide.

The driven barrier failed to provide a tight seal at high surface pressures. It was found that placement of weights on the barrier at the contact with the frame insured a tight seal up to pressures of the order of 25 dynes/cm; but as the pressure increased considerably above this value a space appeared between the barrier and the frame. Improved operation at higher pressures has been obtained with the driven barrier ends placed under the frame and a second strip placed on top of the barrier and the frame, with ends weighted. This causes the frame to be pressed between two barrier strips, forming an effective seal.

The single silk threads supporting the sensing barrier were replaced by multi-strand silk threads, heavily vaseline coated. The stainless steel pins driving the barrier were replaced by quartz rod to enable the use of solutions of low pH. A horizontal brace was added to the torsion

balance frame, with a guide for the shaft of the Langmuir-Blodgett dipping slide holder. Limit switches were installed on the lathe bed to prevent the barrier from being driven either into the end of the trough or into the well area when the motor drive is in operation. A chart recorder was added to the photocell amplifier to provide a visual display and record of the exact position of the control vane attached to the sensing barrier. The chart recorder scale represents a range of about 0.5 dynes/cm, with maximum sensitivity in the center, and less sensitivity at extremes of the range. During film deposition, the automatic control of film pressure is visible as a pen excursion of 1.0 cm, representing a variation in film pressure of slightly less than 0.1 dynes/cm. A potentiometer was connected to the film-compression motor controller, providing continuous proportional control of the speed of the motor during film deposition.

### 2.1.3 Film Building Procedures

When a film of stearic acid is spread on the surface of acidified water and compressed, at a molecular area of about 26.5 Å a "condensed liquid" phase appears. At a surface pressure of 23.5 dynes/cm (molecular area: 22.1 Å) the film is no longer readily compressible; a "condensed solid" phase has been formed. If a film of stearic acid is spread on a substrate containing an alkaline earth cation, such as barium, in solution, the condensed-solid phase forms at low pressures, the pressure and composition being principally functions of the pH of the solution. The shape of the force-area curve, as determined by measurement on the Langmuir trough, indicates the nature of the intermolecular forces.

Initial experiments on stearyl phosphoric acid, in contrast with the results for stearic acid, did not show any evidence of a condensed-solid phase. However, on a substrate containing  $10^{-4}$  molar calcium acetate at pH 9, a change in compressibility was found at a molecular area of about 22.8 Å. Further experiments on more highly purified stearyl phosphoric acid will be found in the Result section of this report.

Samples of pure calcium lechithinate were spread on substrates of distilled water and of saturated calcium hydroxide. No difference was noted; no condensed-solid phase was found as the area per molecule was varied from 105 Å to 70 Å.

A sample of docosanol was spread on the trough; the viscosity of the material was high and it was not possible to obtain equilibrium pressure measurements in a reasonable length of time.

#### 2.1.4 Force-Area Determinations

A solution of the material in a suitable solvent is prepared; for example, 24.75 mg of zone-refined stearic acid was dissolved in redistilled n-hexane to make up 10.00 ml of solution.

The Langmuir trough is cleaned with chromic acid overnight, rinsed thoroughly with running water and then three times with distilled water. The mica frame is coated with fresh paraffin and the silk threads coated with vaseline. Quartz-distilled water is acidified to pH 1.3 (to repress ionization of stearic acid) with sulfuric acid and the trough filled until the water meniscus is visible above the edge of the trough, but not high enough to cause overflowing (about 2 mm). The movable barrier is driven to compress any slight contaminating surface active material to the minimum residual area of the trough. A few milligrams of powdered polyethylene are sprinkled over this residual area, and also over the area behind the sensing barrier. A stream of air from an oil-free pump, filtered through glass wool and bubbled through a water trap, is used to blow the powder and any film to one side of the frame, where it is removed by suction. This cleaning procedure is repeated twice. The movable barrier is then driven to the opposite end of the frame and any film existing on that end removed similarly. The barrier is again driven in the direction of compression to the minimum residual area and the cleaning process repeated. During the cleaning process a small amount of water is removed with the film and powder by the suction; additions of water are made as necessary, but always to the area behind the

movable barrier and with care not to agitate the water unduly. In addition to polyethylene powder, teflon powder and powdered talc were tried. Talc was found to cause measurable contamination due to soluble cations and teflon powder did not give as good sweeping action as polyethylene powder. No evidence of soluble contaminants has been found with either the teflon or the polyethylene powders.

The water surface being thoroughly cleaned, the movable barrier is driven to the opposite end of the frame and the torsion balance adjusted to give a zero reading of 3.0 millivolts on the 10 mv chart recorder scale, halfway between the "on" and "off" positions of the relay controlling the automatic compression motor. An amount of stearic acid solution is placed on the surface from a microliter syringe. The torsion balance is displaced a small degree and the film compression motor started. When the film has been compressed enough so that it exerts a force equal to that of the rotation of the torsion wire, the vane attached to the torsion wire and sensing barrier interrupts the light path to the photocell and shuts off the compressing motor. A few seconds are allowed for equilibrium to be established, and exact readings of the movable barrier position and torsion wire rotation required to bring the chart recorder indication back to 3.0 mv are made. The torsion balance is reset to the next higher pressure and the process repeated until readings have been recorded up to a pressure where film collapse is imminent. In the stearic acid work this process was followed in triplicate with 25.0 microliters of stearic acid solution and again in triplicate with 100.0 microliters of solution. These were graphed and averages taken, and the difference in barrier positions at each pressure between the 100 microliter set and the 25 microliter set was used to calculate the surface area covered by 75 microliters of the solution. Seventy-five microliters of this solution was calculated to contain  $3.93 \times 10^{17}$  molecules of stearic acid; dividing the calculated surface area (in angstroms) by this number gives the area per molecule for each value of film pressure. A graph of these values is included.

#### 2.1.5 Deposition of Barium Stearate

The trough was filled with a solution containing  $2.5 \times 10^{-4}$  molar sodium phosphate buffer at pH 7.0 and  $1.0 \times 10^{-4}$  molar barium acetate. The surface was cleaned, 100 microliters of stearic acid solution added, and compressed to a film pressure of 30 dynes/cm. The slide, cleaned with chromic acid, rinsed in distilled water, coated with ferric stearate and exhaustively rubbed, was lowered by the dipping motor through the film at a rate of about 12 mm/minute. As the slide consumed film, the film compression motor operated to maintain constant film pressure. By measuring the area of the film consumed and comparing this with the area of the slide covered with the film, it was found that the amount of film consumed was equal to the area of the slide covered. When the slide was immersed in the well of the trough as far as possible (the top 4 mm of the slide is covered by a clip and cannot be coated) the dipping mechanism automatically reversed and withdrew the slide; a second layer of film was deposited; the orientation is such that the polar ends of the molecules of each layer are adjacent. The process was repeated to produce films of 43 double layers thickness (2150 Å). A slide 39 mm wide and 50 mm long consumed an amount of film that the trough can supply in 12 double layers; roughly 40 double layers can be applied in a day. After a single film was consumed by the slide the surface was cleaned by suction (but without the use of powder) and a new film spread.

A slide coated with 43 double layers of barium stearate was examined by X-ray diffraction and found to have a highly ordered layered structure with a spacing of 49.3 Å. The first reflection was obtained at an angle of  $1.75^\circ$  and was found to have a very high intensity. Succeeding orders were observed at lower intensities up to  $n = 11$  at  $20.3^\circ$ . Line broadening was nil, indicating a high degree of order or a low concentration of microcrystalline domains. X-ray studies of various lipid like multilayers will be covered in detail in the Result Section of this report.

#### 2.1.6 Multilayer Concentration Cell

A concentration cell was constructed to permit investigation of the electrochemical properties of various

multilayer "crystal" systems (Figure 6). In order to measure the specificity of the barium stearate multilayer as a membrane separating barium chloride solutions, a concentration cell was assembled as follows: glass end pieces constructed with wells for electrode introduction and flat faces for sealing to membrane supports have capacities of about 30 ml of electrolyte. Holes in the face plates 26 mm in diameter provide a large area of contact between adjacent edges of two glass slides. The slides are cemented with epoxy resin to a single 50 mm square of glass with a 26 mm hole in it; this support is identical to the face plates of the concentration cell end pieces. Thus a material for test is exposed to electrolyte solutions on either side of a narrow slit between two pieces of glass. In use the face plates of the end pieces are coated with a thick layer of vaseline, the supported membrane placed between them, and the assembly clamped with heavy rubber bands.

#### 2.1.7 Cell Characteristics

The cell was first assembled without a membrane support to determine the resistance of the electrodes and cell assembly. The cell was filled with 0.1 molar barium chloride solution as electrolyte; silver-silver chloride electrodes were inserted, and the cell resistance was determined with a Keithley 610 electrometer. A resistance of  $3.65 \times 10^5$  ohms was found; no change in resistance was found as the applied current was varied from  $10^{-9}$  amperes to  $10^{-5}$  amperes. Evidently the rate of formation of charge carriers is proportional to applied voltage over this range.

#### 2.1.8 General Protocol for Langmuir-Blodgett Membrane Manufacture

##### Preparation of Substrate:

a. A 2 x 2 inch optical quality glass slide (1mm thick) is scratched with a diamond pencil at the center of one edge and cracked. All slides are discarded that do not have a fairly straight and smooth edge after cracking.

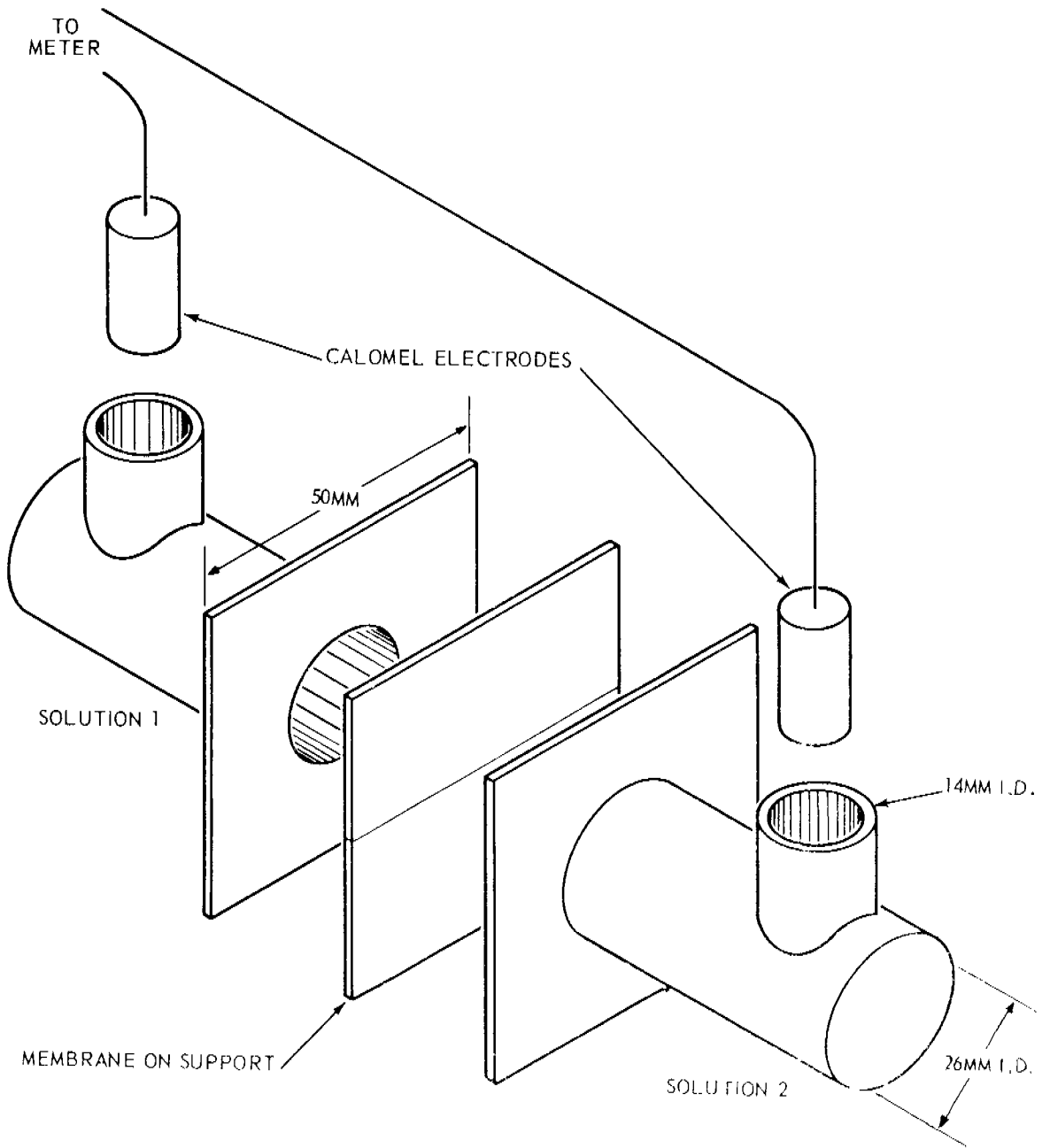


Figure 6. Concentration Cell

b. The slide halves are cleaned in chromic acid, rinsed, dried, and degreased in methanol.

c. The slide halves are made oleophilic either by rubbing with ferric stearate or by dipping in a solution of octadecylamine in nitromethane. It was felt that the second method gave a more uniform monolayer.

d. The slide halves are mounted on clips on the automatic dipping apparatus of the surface balance. The two halves of a single slide are always coated together to insure identical coating composition on the surfaces of each.

### Coating

a. The quartz trough of the surface balance is cleaned with chromic acid, rinsed with distilled water, rinsed with conductivity water, soaked overnight in conductivity water, and rinsed with distilled water, and rinsed in place in the trough with conductivity water and buffer.

b. The trough is filled with sodium phosphate buffered conductivity water of appropriate pH containing  $10^{-4}$  M barium acetate. The surface of the substrate is cleaned by flowing filtered and humidified air across the surface and removing any film collected with vacuum from the other side. Polyethylene powder is used as a sweeping aid. The surface is swept repeatedly. Additional substrate, to bring the level in the trough back to just above the trough edge, is added to the reserve area behind the compression barrier, then both the film preparation area and the reserve area of the substrate surface are swept again.

c. The zero point of the surface balance is determined, and an appropriate quantity of a solution of stearic acid in hexane, (1 to 2 mg/ml) is spread from a Hamilton syringe.

d. The film is compressed to 34 dynes/cm. The final pressure is approached slowly to avoid any possibility of local excess of pressure which might lead to buckling of the film. About 10 minutes at full pressure

are allowed before coating is begun, to allow the solvent to evaporate completely and to insure that pressure equilibrium has been reached throughout the film. In practice during this time the film is seen to compress by 1% or more, with the compression rate slowing as a function of time.

e. The first few layers of film are transferred to the slide at a relatively slow dipping speed (1-2 cm/min) to insure good contact with the prepared slide surface. Later layers are transferred at moderate speeds (3-4 cm/min). Higher coating speeds seem to lead to a cloudy appearance after 50 or more double layers are accumulated. Several minutes are allowed between dips for any residual water to evaporate.

f. After the film available for coating has been consumed, residual film is removed and the substrate surface thoroughly cleaned before a fresh film is applied. For most experiments the frame must be filled three times to provide enough film area to build up the desired number of layers on slides of this size.

### Assembly

a. The slide halves are placed in an aligning jig equipped with an independent "mechanical stage" by which one half may be precisely positioned with respect to the other. The slides rest on another similar, but uncracked, slide surface, and are observed at 100 to 400 power magnification. In practice, since the cracked surfaces are smooth and parallel, much care is required to determine that the surfaces are not displaced. Usually the crack is slightly irregular at the end of the slide that was scratched to begin the crack, and the small projections or chips can be used as aligning guides. Another serious difficulty is the vertical positioning of the slide. Ideally the slide should lie flat on the optically smooth reference slide, but in practice they may not meet perfectly, perhaps as a result of specks of dust between the slide and the reference surface, and perhaps resulting from support of the slide by the alignment clamps. Generally a gentle finger pressure downwards is sufficient to bring the slides into good, though not perfect, alignment.

b. The slide halves are moved together stepwise by the mechanical stage adjustment, checking alignment along the back at each step. When alignment is satisfactory, the slide halves are pushed firmly together with the mechanical stage adjustment. Usually a slight lateral or vertical motion is visible through the microscope as the slides meet, accomplishing the final exact match of the surfaces. Occasionally the slide halves fail to meet perfectly, leaving a wide crack visible under 400 X magnification. Fifty double layers of barium stearate should amount to a filled crack 0.25 microns wide, or appearing as 0.1 mm wide after 400 X magnification.

c. The alignment jig is removed from the microscope and a cover slide with a circular hole for membrane access is cemented on with epoxy resin. This is allowed to dry overnight, and the assembly is removed from the jig, turned over, and another cover slide cemented to the other side. This is allowed to dry overnight, and the completed assemblies stored in a dust-free file until ready for use.

#### Assembly of the Conductivity Cell

a. The surfaces of the cover slides are cleaned carefully with methanol, wiped with dust-free tissue, and coated with petroleum jelly as a sealant material.

b. The membrane assembly is then clamped between thermostated Teflon half-cells.

c. Electrolyte solutions containing either 0.01 M or 0.1 M barium chloride are introduced into the cell chambers, and silver-silver chloride electrodes are inserted. The entire assembly is placed in an insulated, shielded box and the thermostated water circulation turned on.

#### DC Measurements

a. The Keithley model 610 meter is attached to one electrode of the cell and the other electrode grounded. The potential of the electrode is measured, the electrodes reversed, and the potential measured again.

b. Beginning at the  $10^{-12}$  ohm range, the Keithley electrometer is switched to measure the cell resistance. If the cell potential found is close to zero the meter is adjusted to read zero with the meter zero adjustment before resistance is measured; otherwise the cell potential can be subtracted from the apparent resistance to obtain the true resistance. Resistance is determined using each range of the meter up to a maximum voltage impressed across the cell of 1 volt. From the several readings a best value can be estimated. The electrodes are reversed and the process repeated to obtain the resistance from the other side. The two values should be equal, any difference indicating a leakage path external to the membrane.

c. It has been found that membranes with DC resistances greater than about  $10^{12}$  ohms do not yield a reproducible cell potential.

d. Membranes are tested as reversible electrodes by placing a 0.1M barium chloride solution in one chamber of the cell and a 0.01 M solution in the other. A concentration cell potential close to the theoretical potential of 74.1 mv indicates a functioning membrane. In practice the solutions must be reversed several times to bring the membrane to equilibrium and determine the extent of membrane asymmetry and polarization (usually a few mv).

#### AC Measurements

a. The electrodes of the cell are connected to the "3-terminal" bridge terminals of the GR 1615 conductance-capacitance bridge, the meter sensitivity increased until the background electrical noise is just measurable (less than 10% on the meter scale), and the audio oscillator output voltage increased slightly and a frequency is selected. The tunable filter on the meter is adjusted to maximize the meter reading at this frequency. The first one or two significant figures of the capacitance may then be dialed on the bridge decade switches. Thereafter, conductivity and resistance decades are adjusted alternately until a satisfactory null is achieved.

b. The process is repeated for each frequency of interest. Duplicate determinations are made after a ten minute interval.

c. Immediately after completing measurements at one temperature, the thermostat bath temperature is raised as quickly as possible ("high heat") to the next temperature. Ten minutes are allowed for the cell to approach thermal equilibrium and a new set of conductance-capacitance-frequency measurements made. A duplicate determination ten minutes later is usually quite close, indicating that the first measurement was close to the equilibrium value, and that the second one is adequately close.

d. The membranes are ordinarily not cycled to above 50°C, since membrane deterioration seems to be more rapid at higher temperatures.

e. After completing measurements at 50°C, the thermostat bath may be cooled in 1° increments. Appreciable hysteresis is usually found in this cycling, suggesting that even though thermal equilibrium seems to be achieved, hydration equilibrium may be slower.

f. Attempts have been made to cool the cell below room temperature. It has been found that abrupt increases in the measured conductance occur below about 15°C. Even when the cell is swept with dry helium gas the results are not reproducible.

## 2.2 Cast Membranes

### 2.2.1 Preliminary Remarks

Several membranes have been prepared by solvent evaporation from solutions spread on the surface of a glass plate using a doctor knife. Sodium stearate is compatible with the acetone solvent of commercial Collodion (Fisher, U.S.P.) and has been used to form the center layer of a tri-layer, Collodion - Sodium Stearate - Collodion film. Another approach consisted of a solvent extraction and crystallization of commercial "Parafilm" to remove the excess

paraffinic plasticizer which was then replaced with stearic acid. This system was then used as the center membrane of a Collodion - "Polyisobutylene" - Collodion film. A third approach consisted of forming a film of insolubilized polyvinyl alcohol containing potassium stearate.

These systems did not exhibit permselective activity or had undesirable physical properties. The stearic acid-polyisobutylene and the sodium stearate-collodion membrane systems were eliminated under these conditions. The stearic acid-polyisobutylene membrane was water nonwetttable and the sodium stearate-collodion system had a tendency to swell and part into two pieces (delamination).

#### 2.2.2 Preparation of Potassium Oleate-Collodion Membranes

Four grams of potassium oleate and 1 milliliter of water were added to 50 ml of commercial collodion (Baker). This mixture was warmed to dissolve and solubilize the soap. After cooling to room temperature, the mixture was centrifuged and the clear supernatant was decanted into a stoppered bottle.

A typical preparation was converted to a suitable membrane in the following manner. A clean glass plate (8 x 8 inches) was coated with 4 layers of commercial collodion solution by means of a 0.003-inch doctor's knife. About 10 minutes were allowed between the application of successive layers to permit drying. Each layer was then relatively free of the acetone-ether solvent. The soap-collodion solution was layered, using the same technique. A longer drying time was required for this layer because of the small quantity of water added to the solution. After the third soap-collodion layer was applied, the membrane was allowed to dry for about an hour before the final four coats of pure collodion were applied.

#### 2.2.3 Preparation of Collodion-Polysoap Membranes

Polysoaps were synthesized according to the method given by Medalia, et al<sup>2</sup>. Two types of polysoap were successively synthesized; one by the alkylation of Dow PS-2

polystyrene (mol. wt. = 20,000) and the other by the alkylation of Dow PS-3 polystyrene (mol. wt. = 50,000). Methyl oleate was used in both instances.

Attempts to prepare the membrane by dissolving the polysoap in the collodion solution were unsuccessful. This was probably due to the limited solubility of the polysoap in the ether-acetone solvent. Membranes were prepared by casting a 10 percent aqueous polysoap solution on a three-layer collodion membrane or by casting a 10% polysoap solution in  $\text{CH}_3\text{OH}$  on a collodion surface (also in  $\text{CH}_3\text{OH}$ ). A variable number of layers of collodion were then cast over the dried polysoap layers.

### Collodion

In the endeavor to control porosity, stock collodion solutions were prepared by dissolving Mallinckrodt Parlodion (a purified pyroxylin) in a suitable solvent. Methanol, acetone and ether were employed in the solvent studies.

### 2.3 Membrane Nomenclature

PS 3-2-2-2 identifies the membrane as consisting of two layers of collodion, a, - two layers of potassium polysoap, b, - and, two layers of collodion, c, - in that order. PS 3 relates to the origin of the polysoap; Dow polystyrene, No. 3, Mol. Wt. 50,000.

### 2.2.4 Determination of Membrane Properties

The cells used for the studies reported here were of the detachable "U" tube type. These cells were constructed of two cylindrical glass tubes joined together by means of an "O" ring glass joint at right angles to the body of each tube. The membrane to be studied was inserted between the two "O" ring glass joints and held firmly in place by means of a ball and socket clamp.

Potential measurements were made using a Keithly Model 610 A electrometer. Beckman sealed calomel electrodes were used in both of the electrode compartments. Shielded

cable was used between the electrodes and the electrometer. Bi-ionic or concentration cell potentials were recorded after a constant voltage reading was obtained. This equilibration time varied from 5 to 30 minutes.

The electrode asymmetry was determined by two independent methods: by placing the electrodes in an equimolar salt solution; and by reversing the electrodes in each half of a membrane cell. The difference between the two readings obtained by the second procedure is equal to twice the electrode asymmetry determined by the first procedure.

An Industrial Instrument Model No. RC-18 conductivity bridge was used in the diffusion studies. Since suitable commercial conductivity cells were not available, special dipping conductivity cells were constructed using platinum electrodes 1.5 cm in diameter and spaced 3 cm apart. The platinum electrodes were coated with platinum black to minimize the effects of polarization.

Electrolyte was allowed to diffuse from the concentrated region to the cell chamber containing 90 ml of triple-distilled water. The dipping conductivity cell was immersed in the distilled water. The diffusion apparatus was then placed in a constant-temperature bath set at 25°C. The electrolyte concentration was usually 1.0 molar and bridge readings were taken every 5 minutes. A magnetically driven stirring bar was placed in the distilled water chamber of the apparatus. The cell constant was determined by measuring the conductivity of 0.1 and 0.2 molar KCl solutions.

### 3. RESULTS

#### 3.1 Langmuir-Blodgett Techniques

##### 3.1.1 Effect of Orientation on Selectivity

A membrane was formed of barium stearate melted into a crack between two glass slides in order to compare the properties of a randomly oriented material with that of the oriented single crystal. It was mounted in the concentration cell in the same manner, but the membrane cross-sectional area was considerably larger. The space between the glass slides, filled with barium stearate, was visible under the microscope as a band several microns wide. The resistance of this membrane placed in the concentration cell with 0.1 M barium chloride solutions on both sides was  $2.9 \times 10^6$  ohms. With a 0.1 M barium chloride solution on one side and a 0.2 M solution on the other, a potential of 18.5 mv was developed across the membrane, as compared with a theoretical calculated potential of 22.15 mv<sup>3</sup>. It appears that some ion-conductive pathways exist in the polycrystalline membrane, but not enough to develop the full potential expected. On reversal of the solutions about the membrane, this potential dropped to 4.5 mv but did not reverse in sign. On reversing the solutions again, the potential developed slowly rose to the initial value of 18.5 mv.

##### Paraffin Membrane

A membrane was formed of paraffin melted between edges of two glass slides. A resistance of  $2.6 \times 10^7$  ohms was found when this membrane was placed between solutions of 0.1 M barium chloride. When the membrane was placed between 0.2 M and 0.4 M electrolytes, a potential of 3 mv was found.

##### Ferric Stearate

A membrane was similarly formed of ferric stearate. A resistance of  $1.2 \times 10^6$  ohms was found when the membrane was placed between 0.1 M barium chloride solutions. When the membrane was

placed between 0.02 M and 0.04 M solutions of barium chloride, reproducible values of the potential between the solutions could not be obtained; an apparent membrane resistance of  $2 \times 10^{10}$  ohms was found.

### Millipore Filter

A millipore membrane with a single layer of barium stearate deposited on each side was placed between the end pieces of the concentration cell. No increase in cell resistance was found, so it is assumed that defects existed in the deposited layers rendering them porous.

### 3.1.2 Multilayer Structure Formation of New Materials

Barium stearate has been used in most of the studies because of the large amount of backup data and surface chemical technology associated with this substance. However, it was desirable to attempt to improve the properties of the multilayer surface in two ways: (1) increase the degree of order in the "crystal", which can be done by using longer hydrocarbon chain ionic lipids; (2) increase the resemblance of the multilayer structure to biological structures by using materials found in natural membranes, e. g. , lecithin. The following paragraphs describe studies designed to fulfill these two aims.

#### Cerotic acid

Force-area curves were determined for films of cerotic acid,  $C_{26}H_{52}O_2$ . (Figure 7) This was chosen as an extremely long-chain acid with a melting point ( $87.7^\circ C$ ) higher than that of stearic acid ( $69.4^\circ C$ ). A condensed phase similar to that of stearic acid was found, but film collapse did not occur below 55 dynes/cm.

When a glass slide coated with ferric stearate was dipped through a film of cerotic acid at pH 1.3, a double layer of film could be deposited, but additional dipping of the slide through

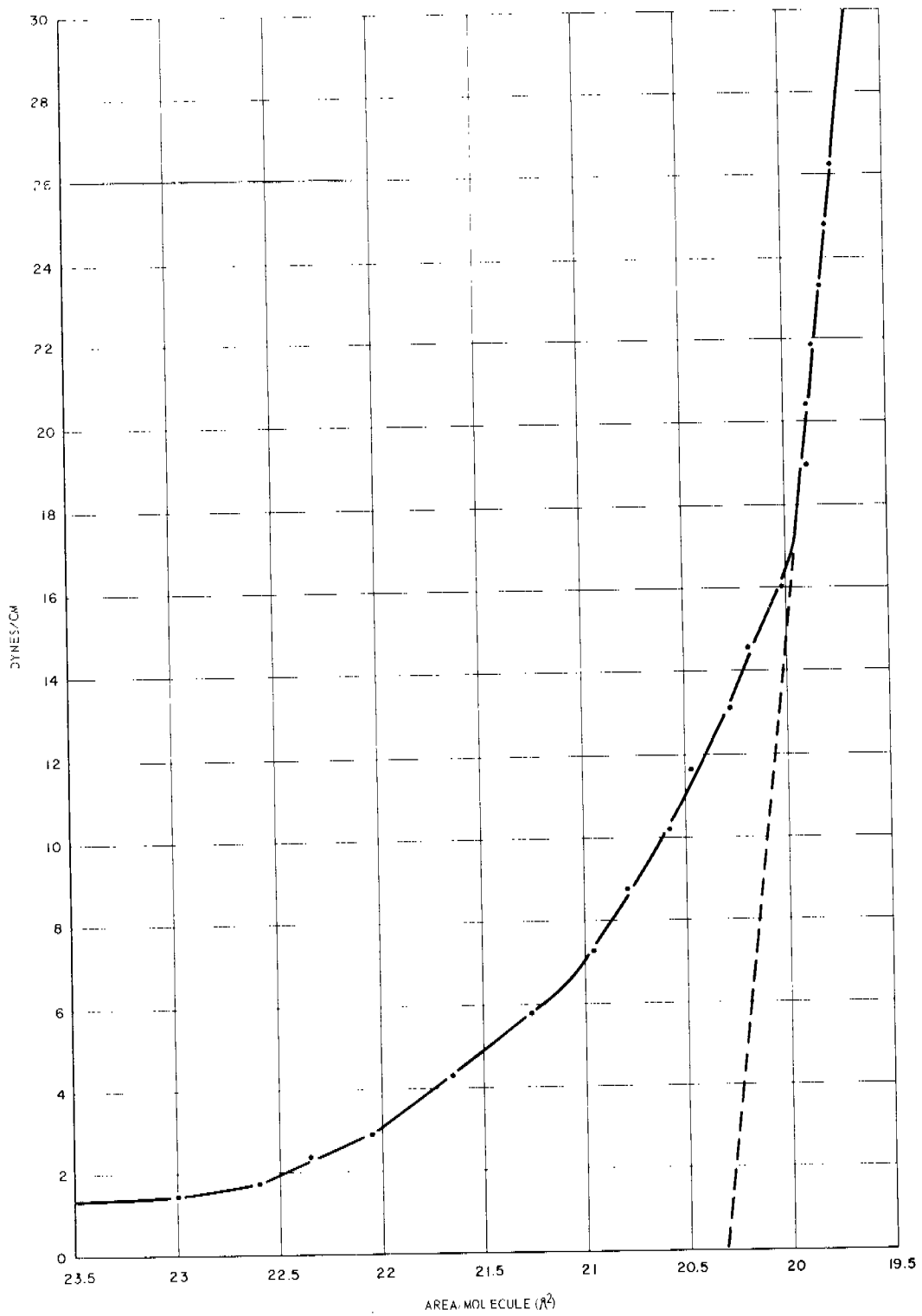


Figure 7. Force-Area Curves of Cerotic Acid on pH 1.3 Substrate

the film failed to produce a multilayered structure. The hydrophobic layer, deposited as the slide was raised, spread, on reimmersion, from the slide onto the water surface even against a surface pressure of more than 30 dynes/cm. The trough was filled with a substrate containing  $10^{-4}$  M barium acetate and  $2.5 \times 10^{-4}$  M sodium phosphate buffer at pH 3.5, and a glass slide coated with ferric stearate was dipped through the compressed film. It was possible to coat the slide with more than one double layer of the mixed cerotic acid-barium cerotate film, but the film deposited was uneven and appeared to have only wet the slide in some areas, leaving the slide only partially coated. The substrate was replaced with one of pH 6. A ferric stearate-coated slide dipped through a compressed film (30 dynes/cm) passed through the film without removing film from the water surface. At pH 6.8 it was found that film was transferred to the slide only on the upstroke. Langmuir and Blodgett called this a "Z" type of film. A similar result was obtained on a pH 9 substrate: film was transferred to the slide only on the upstroke. The slide was not perfectly covered in this case either and appeared streaked. A millipore filter sheet did not remove any film from the surface of the water on either stroke of the dipping apparatus. The barium cerotate films formed seemed generally to be viscous; that is, on compression or expansion of the film, pressure equilibrium throughout the film may take several minutes to be achieved. As a result, film must be transferred from the trough surface extremely slowly, since rapid transfer will result in depletion of film in the area around the slide but the resulting low film pressure may take minutes to become sensed by the barrier. From the practical standpoint, it appears that it will be difficult to prepare multilayer structures from a fatty acid as long as 26 carbon atoms.

### Lecithin

Lecithin micelles have been found to exhibit differential solubilizing power for sodium and potassium dye salts. Lecithin salts in the presence of water are hydrated but not soluble. A multilayer structure of oriented lecithin molecules would present an ideal system for the study of monovalent cation-phospho-lipid interaction.

Lecithin solution in petroleum ether was spread on substrates containing  $10^{-4}$  M barium acetate at pH 6.6 and at pH 9.9. At about 19 dynes/cm the film seemed to become considerably less compressible. (Figure 8) A slide, previously coated with 8 double layers of barium stearate to provide an oleophilic surface was dipped through the film. Lecithin film was transferred to the slide on the downstroke, but on the upstroke the film returned to the surface of the water even at surface pressures of 39 dynes/cm rather than forming a double layer. It has been reported in the literature that addition of cholesterol to a lecithin film leads to a contraction of the film. To investigate the possibility that cholesterol might significantly affect the surface properties of a barium lecithinate film, an amount of cholesterol approximately equal in weight to the amount contained lecithin was added to a lecithin solution and spread to a pH 9.9 substrate. No change in the force-area was found. An oleophilic slide dipped through the film consumed film on the downstroke, but returned it to the surface on the upstroke exactly as the cholesterol-free film.

### Cephalin

The cephalin molecule, in basic solution, contains a terminal amine group on the polar end, rather than the terminal quaternary ammonium group of lecithin. The polar end being uncharged may be less strongly bound to the water surface than might lecithin, and may be deposited to form a multilayer structure.

A force-area curve was prepared on a sample of cephalin (synthetic, chromatographically homogeneous L- dipalmitoyl) (Figure 8). The curve of cephalin was similar to that found for lecithin but showed lower compressibility on a pH 9.4 sodium phosphate-buffered substrate  $10^{-4}$  M in barium acetate. A barium stearate-coated slide was dipped through the film at 35.4 dynes/cm surface pressure. Film was transferred to the slide both on the downstroke and on the upstroke. On redipping the top layer was found to leave the slide and return to the surface of the water even against a surface pressure as high as 52.5 dynes/cm. Force-area curves on stearic acid and stearyl phosphoric acid (Figure 9) and on calcium lecithinate and calcium stearyl phosphare (Figure 10) were also obtained.

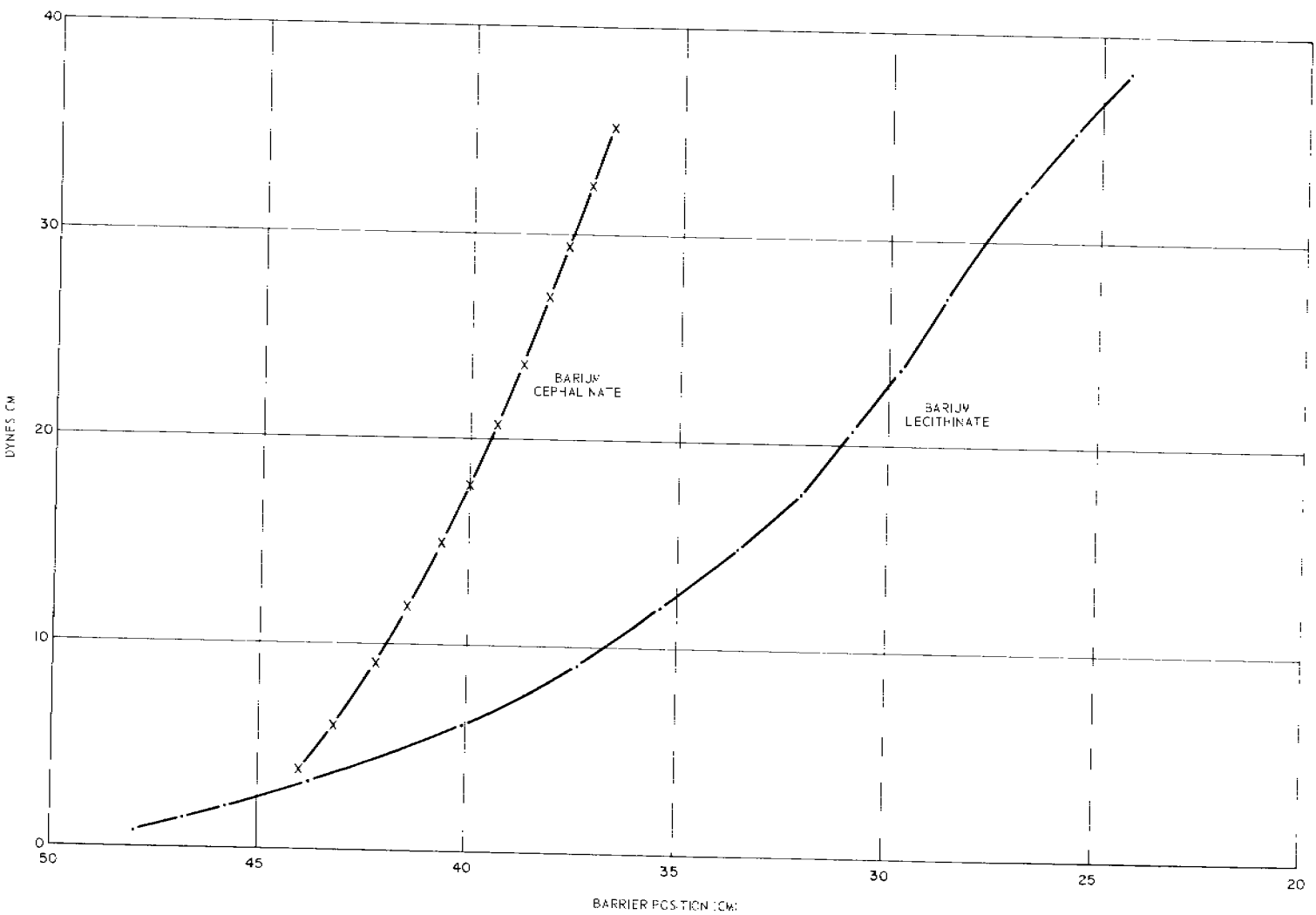
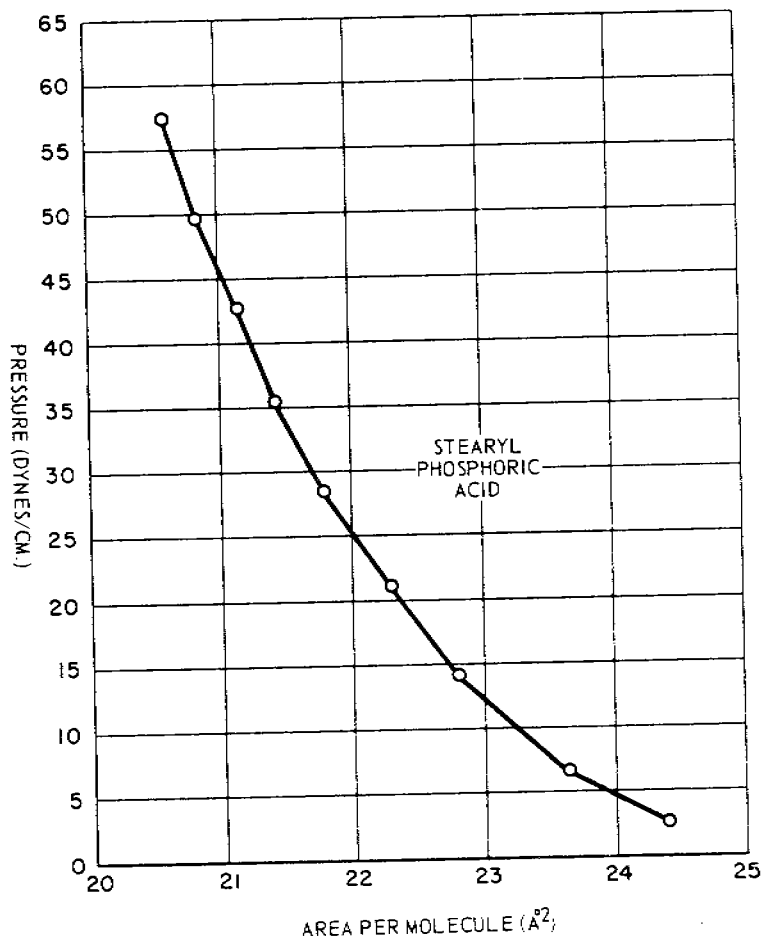
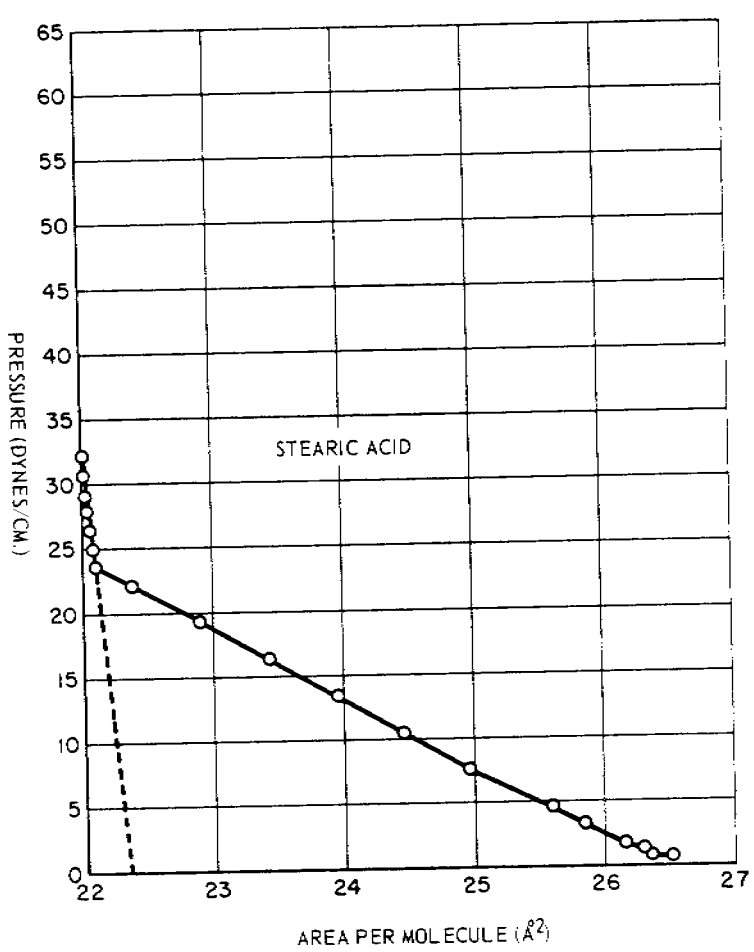


Figure 8. Force-Area Curves of Lecithin and Cephalin Films on Barium-Containing Substrate

Figure 9. Force-Area Curves of Stearic Acid and Stearyl Phosphoric Acid



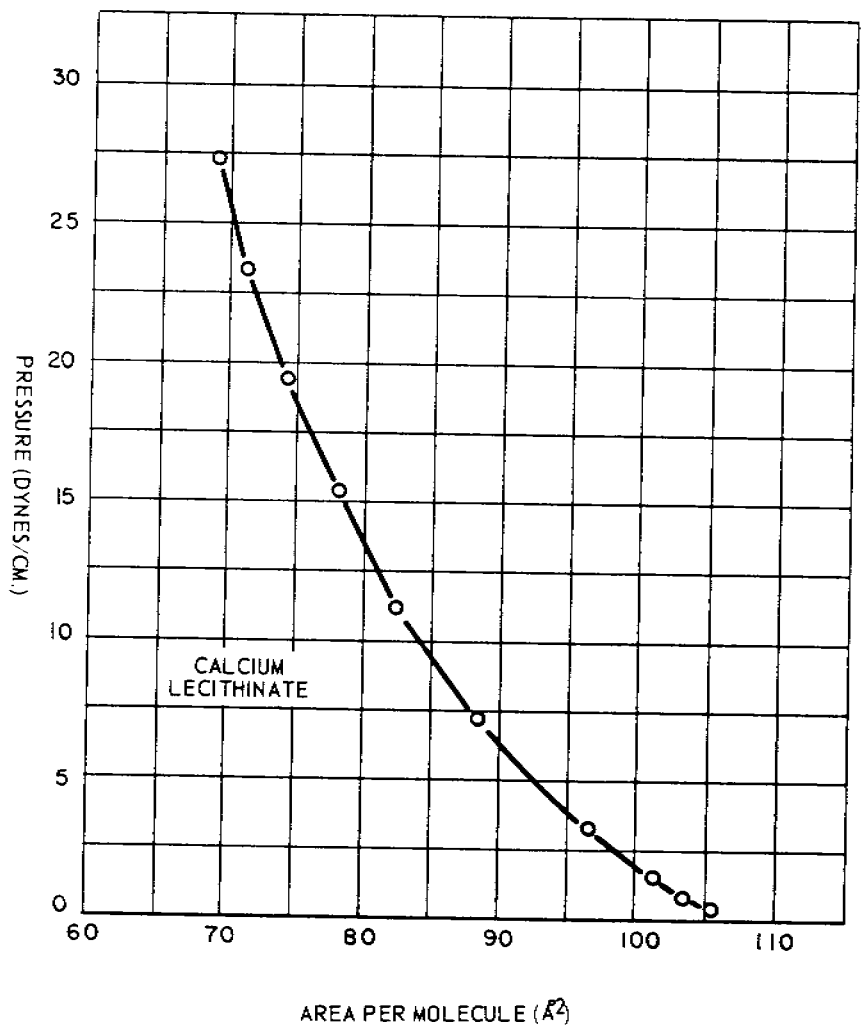
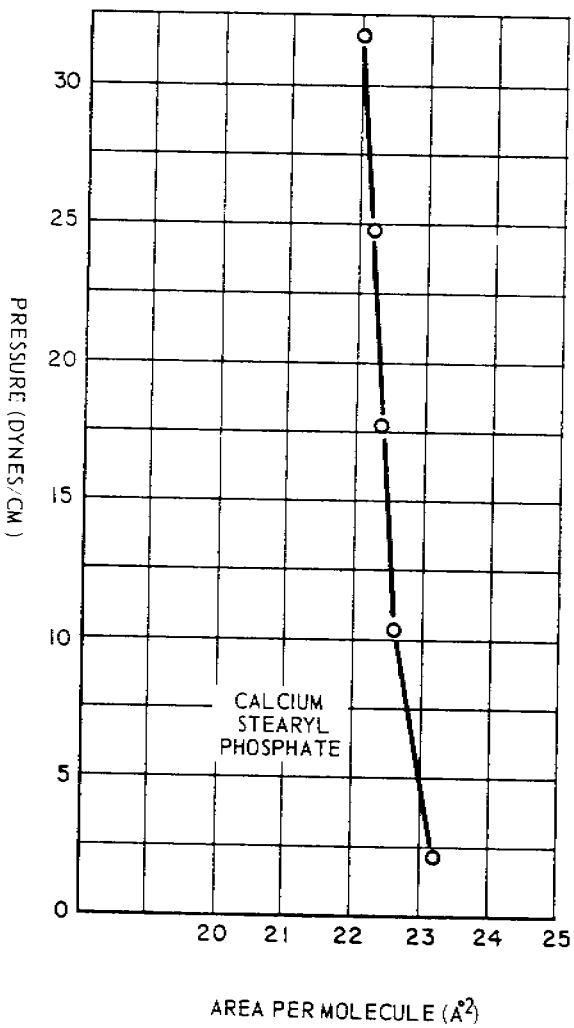


Figure 10. Force-Area Curves of Calcium Stearyl Phosphate and Calcium Lecithinate

### 3.1.3 Formation of Barium Stearate Structures and Effects of Pressure

The surface pressure at which the barium stearate is held during film formation was expected to influence the degree of order of the deposited multilayer structure. Therefore, films were compressed to several different pressures from that at which the film became liquid-condensed, up to the vicinity of the pressure of film collapse.

Stearic acid was spread on a substrate containing  $10^{-4}$  M barium acetate and  $2.5 \times 10^{-4}$  M of pH 7.5 sodium phosphate buffer. The film was compressed to a surface pressure of 18.7 dynes/cm, and a glass slide coated with ferric stearate was rubbed and dipped through the film. Film was deposited on the slide on the downstroke (into the water) but partially came off on the upstroke (removal from the water). At a film pressure of 20.1 dynes/cm, coating of the slide was better but the surface was not perfectly covered. At 21.6 dynes/cm one side of the slide coated well but film came off the other side on the upstroke. At 39.1 dynes/cm, the surface of the slide in air had a rough appearance after dipping, as though some water was included under the film or the film was collapsing irregularly during deposition. Two slides were coated for analysis by X-ray diffraction with 33 double layers each of barium stearate at film pressures of 25.0 dynes/cm and 35.2 dynes/cm. In this pressure range the coating appeared to be free of defects.

### 3.1.4 Effect of Dipping Rate

At rapid dipping rates, visible defects are found in the multilayer structure. To evaluate the effect of these on the interplaner order of a barium stearate multilayer, a slide was coated at the maximum dipping rate of the Langmuir-Blodgett apparatus and analyzed for relative intensity and broadening of the X-ray diffraction from the 49.3 Å interplaner spacing.

This slide was coated with 33 double layers of barium stearate at a film pressure of 35.2 dynes/cm at a very fast dipping rate, about one double layer per minute (5 cm/min). Some defects in

the coated surface appeared, as in previous experiments, producing a slightly cloudy appearance. Under the microscope, individual particles could be distinguished.

1.75° X-ray Diffraction Peak Intensity of Barium  
Stearate Multilayer Crystals Prepared Under Different Conditions

Slide Con- dition:				Irradi- ated	Forty-three double layer multilayer slide aged 2 months
Surface Pressure:	35 dynes/ cm	35 dynes/ cm	25 dynes/ cm	25 dynes/ cm	
Rate:	Slow	Fast	Slow	Slow	
Peak in- tensity (cpm $\times 10^5$ )	3.5	1.96	3.2	1.12	0.35
Half width ( $\text{\AA}$ )	1.45	1.69	1.49	1.64	2.07

3.1.5 Effect of Copper Ion

Blodgett found that coating speed could be improved by adding small amounts of copper ion to the substrate solution. Accordingly, a substrate solution was prepared containing  $10^{-6}$  M copper acetate,  $10^{-4}$  M barium acetate, and  $2.5 \times 10^{-4}$  M sodium phosphate buffer at pH 7.0. A slide coated with a monolayer of ferric stearate was dipped through a stearate film formed on this substrate and coated evenly at the maximum dipping velocity, 5 cm/min. Some roughness in the coating was noted after some 40 double layers were deposited, but dipping was continued until 100 double layers were deposited with reasonable uniformity. This slide was not analyzed by X-ray diffraction, but as intended for use in a concentration cell experiment.

The pH is known to affect the proportion of stearate present in the film, but the effect of this on crystal spacing and crystal order (as measured by broadening of the X-ray diffraction peak) has not previously been measured.

Another slide for X-ray analysis was coated with 33 double layers of barium stearate at a film pressure of 32.8 dynes/cm and a substrate pH of 6.6. At pH 6.6 the film has been found<sup>4</sup> to contain about 50% barium stearate and 50% stearic acid, while at pH 7.5 the film has been found to contain about 70% barium stearate and 30% stearic acid. The crystal spacing and peak width found on analysis by X-ray diffraction were identical to those of samples prepared at pH 7.5, but the peak intensity was lower. This slide was heated to a temperature of 70° C (the melting point of stearic acid is 69.4° C) and a gradual, irreversible recrystallization followed. (Figure 11). A partially crystalline structure could be seen under the microscope after the slide was returned to room temperature.

The structural characterization of the barium stearate multilayer by X-ray analysis required a standard of reference. Barium stearate precipitated from solution with the appropriate stoichiometry was chosen for this standard. The experimental approach to obtaining data for structural comparisons was to measure X-ray diffraction of multilayer and polycrystalline material as a function of temperature.

Powdered barium stearate was spread on a Vaseline-coated aluminum plate, which was then mounted in a Siemens X-ray diffraction apparatus. Peaks were found which correspond in position with those of the multilayer structure, but considerable difference in the relative heights of peaks were found. (Figure 12)

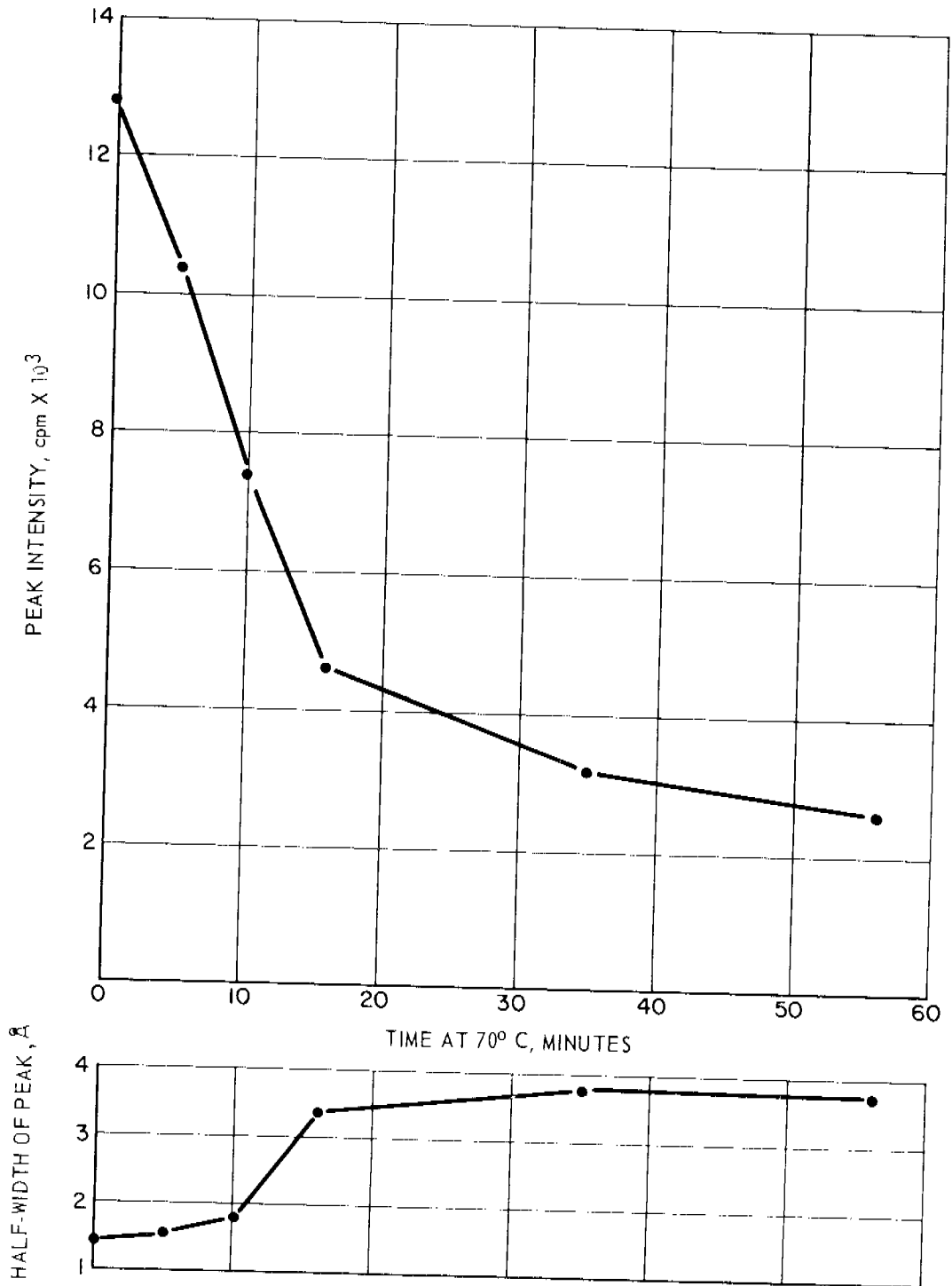


Figure 11. Recrystallization Changes on X-Ray Diffraction Peak from  $49.3\text{\AA}$  Crystal Spacing of Barium Stearate Multilayer at  $70^{\circ}\text{C}$

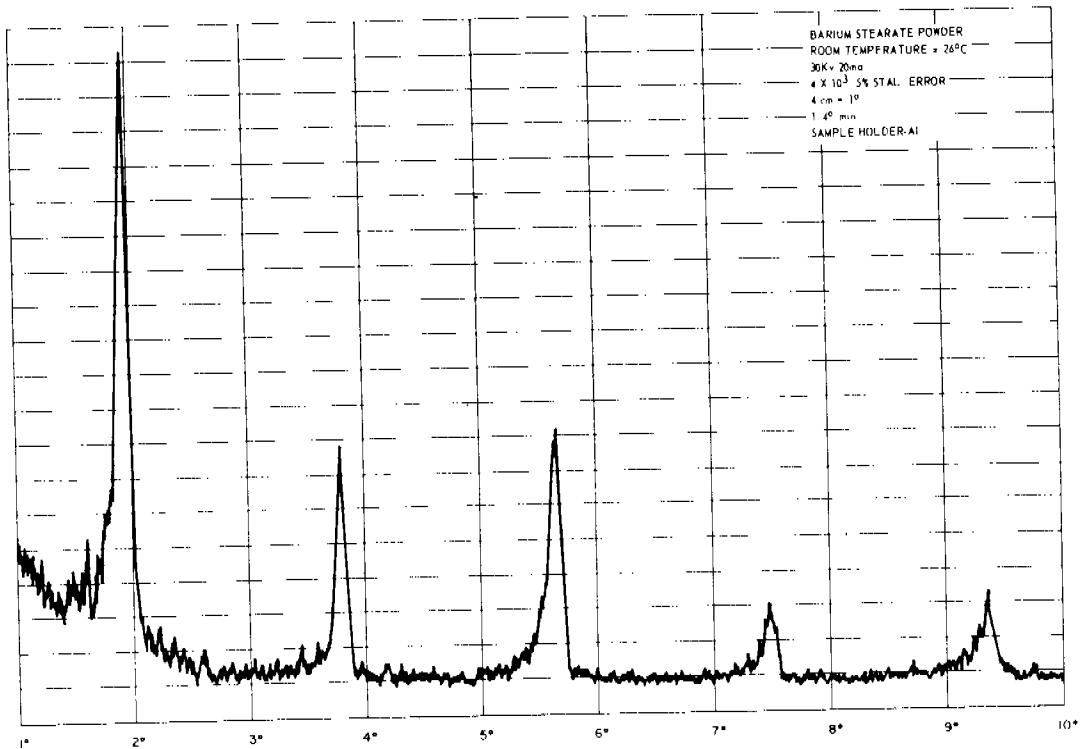
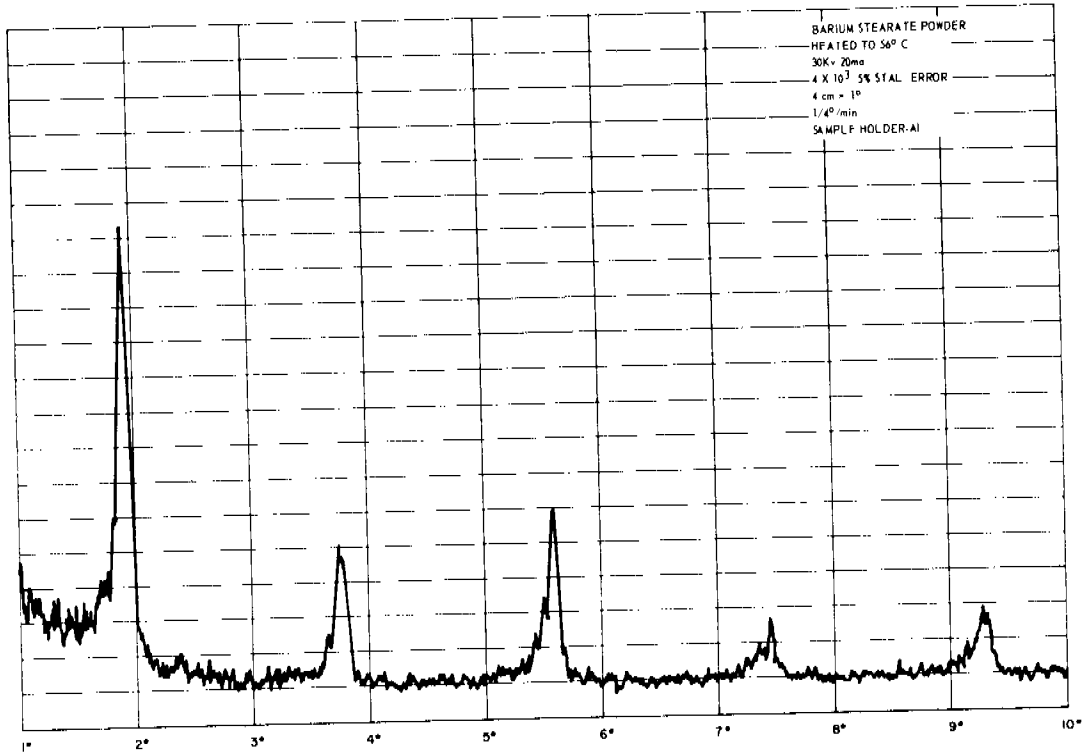


Figure 12. Long Spacing of X-Rays from Polycrystalline Barium Stearate  
CuK $\alpha$  Radiation

While the multilayer structure produced a peak intensity corresponding to a 49.3 Å spacing about 20 times the intensity of the 25 Å peak, the ratio for the powdered material is only about 3.1. The 25 Å starting peak intensity is about 10 times that of the 10 Å peak in the multilayer structure and about three times in the powdered material.

Response to increased temperature (increased thermal motion of the hydrocarbon tails in the multilayer structure) was expected to be manifested in X-ray diffraction analysis as a change in crystal spacing, a peak broadening, or a change in intensity of the reflection.

A barium stearate multilayer of 43 double layers (formed at 30 dynes/cm surface pressure on a pH 7.1 substrate) was exposed in the X-ray diffraction apparatus on a heated sample holder. (figure 13). Curves were run through the principal peak at 1.75° (49.3 Å crystal spacing) at sample temperatures of 28°C, 48°C, 68°C, then again at 29°C. (Figure 14). The spacing did not shift in this temperature range, but the peak intensity did drop with increase of temperature, reversibly, as follows:

1.75° X-ray Diffraction Peak Intensity of Heated  
Barium Stearate Multilayer Crystal

Temperature	28°C	48°C	68°C	29°C (after heating)
Peak Intensity	15.5	11.2	9.7	18.5

(arbitrary units)

No line broadening occurred. A similar run on powdered barium stearate showed no change in peak intensity of 36° and 46°C, but a drop of 56° to a peak intensity of 11.2 (same arbitrary units).

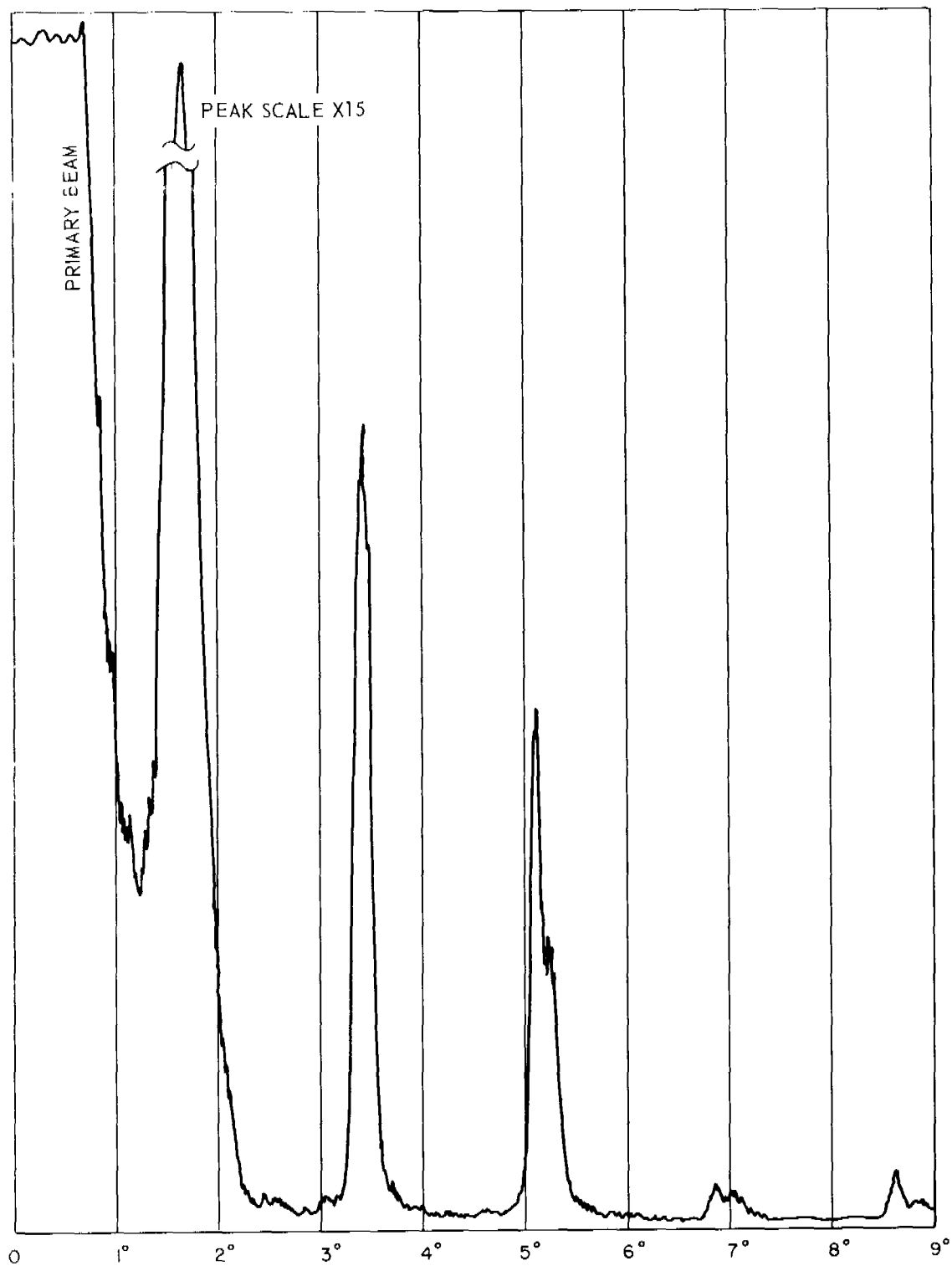


Figure 13. Long Spacing Reflections of X-Rays from Barium Stearate Multilayer

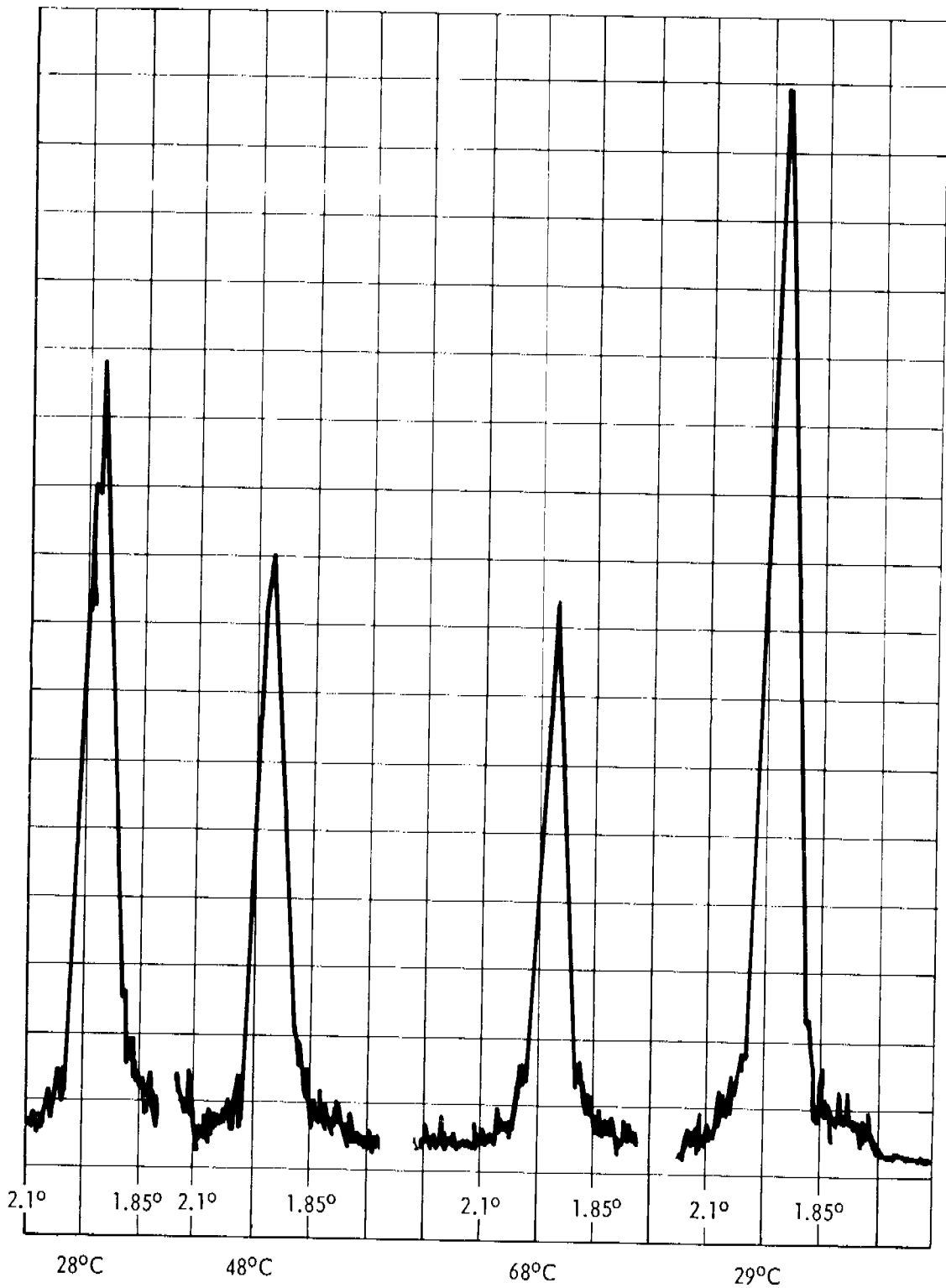


Figure 14. X-Ray Diffraction Curves of Principle Peak ( $1.75^\circ = 49.3\text{\AA}$ ) of Barium Stearate Multilayer Heated to Several Temperatures

### 3.1.8 Barium Stearate Multilayer - Effects of Irradiation

The 25 dynes/cm slide was irradiated with CuK radiation overnight (12 hours) at a maximum beam intensity. The intensity was seen to drop approximately one-half, and a slight line broadening was evident. The irradiated area of the slide was visibly darkened. This result sets obvious limits on the time allowed for irradiation.

### 3.1.9 Adhesion to Glass

Since the multilayer-membrane cell is designed to use multilayers prepared on the edge of a slide, several attempts were made to coat the bottom edge of a slide, i. e. , the surface first presented on a dipping into the water. It was found that this surface would not be coated on entry into the water, even if it were previously coated with barium stearate. The surface layer was removed from the bottom edge of the slide to the surface of the water on dipping into the water through a barium stearate film. It was concluded that the film must be deposited on a surface perpendicular to the surface of the water to obtain adequate adhesion. An attempt was made to deposit barium stearate onto a glass slide without the use of a rubbed layer of ferric stearate. A glass slide, cleaned and degreased, was lowered into the trough through a cleaned water surface, free of film. The water contained  $10^{-4}M$  barium acetate and  $2.5 \times 10^{-4} M$  of sodium phosphate buffer at pH 7. Then stearic acid solution was added to the surface of the water and the film compressed to 30 dynes/cm. On removal of the slide from the trough, film was deposited onto the glass, but on reimmersion of the slide the film returned to the water surface film. At 36 dynes/cm and a fairly rapid dipping speed some film was picked up on reimmersion of the slide through the film, but the surface appeared to be covered unevenly.

### 3.1.10 Adhesion to "Millipore" Filter Material

If oriented barium stearate layers can be deposited on a porous support with the plane of the layers parallel to the surface of the support, then the properties of the crystal structure normal to the planes can be compared with the properties measured in the plane.

It was found that a millipore filter sheet precleaned with petroleum ether and dipped through a compressed barium stearate film would be coated only on withdrawal from the trough; thus a single layer only is deposited on each side of the filter sheet. If the filter sheet is dipped without being washed in petroleum ether, film is deposited on both strokes of the dipping apparatus; thus a double layer is deposited on each side of the filter.

### 3.1.11 Membrane Characteristics

Work during the first part of the contract period using X-ray diffraction, showed that no significant structural changes occurred in barium stearate multilayers in the temperature range 25°C to 68°C. These results are summarized in Figure 15. This method of analysis is only capable of detecting changes in interlayer spacings which depend upon gross changes in position of the long lipid chains of the fatty acid; it reveals nothing about changes that may occur in the polar sheets. Even though no X-ray detectable changes in structure could be found, previous work of a preliminary nature indicated that conductance changes occurred in heated multilayer membrane systems. These could be interpreted as being related to changes in polar sheet structure not detectable by X-ray diffraction. Therefore, the emphasis of the studies on structural

changes in the multilayer system was shifted from direct structural probing using X-ray diffraction, to an indirect approach aimed at detecting changes in the conductance process as a function of temperature.

Measurements of conductance of the barium stearate multilayer membranes were made over the range of 25°C to 68°C by standard AC and DC bridge methods. The upper temperature was just below the melting point of stearic acid. Reference experiments in the case of AC conductance measurements consisted of similar measurements with and without glass slides between solution reservoirs and also using synthetic ion exchange membranes. Because of the

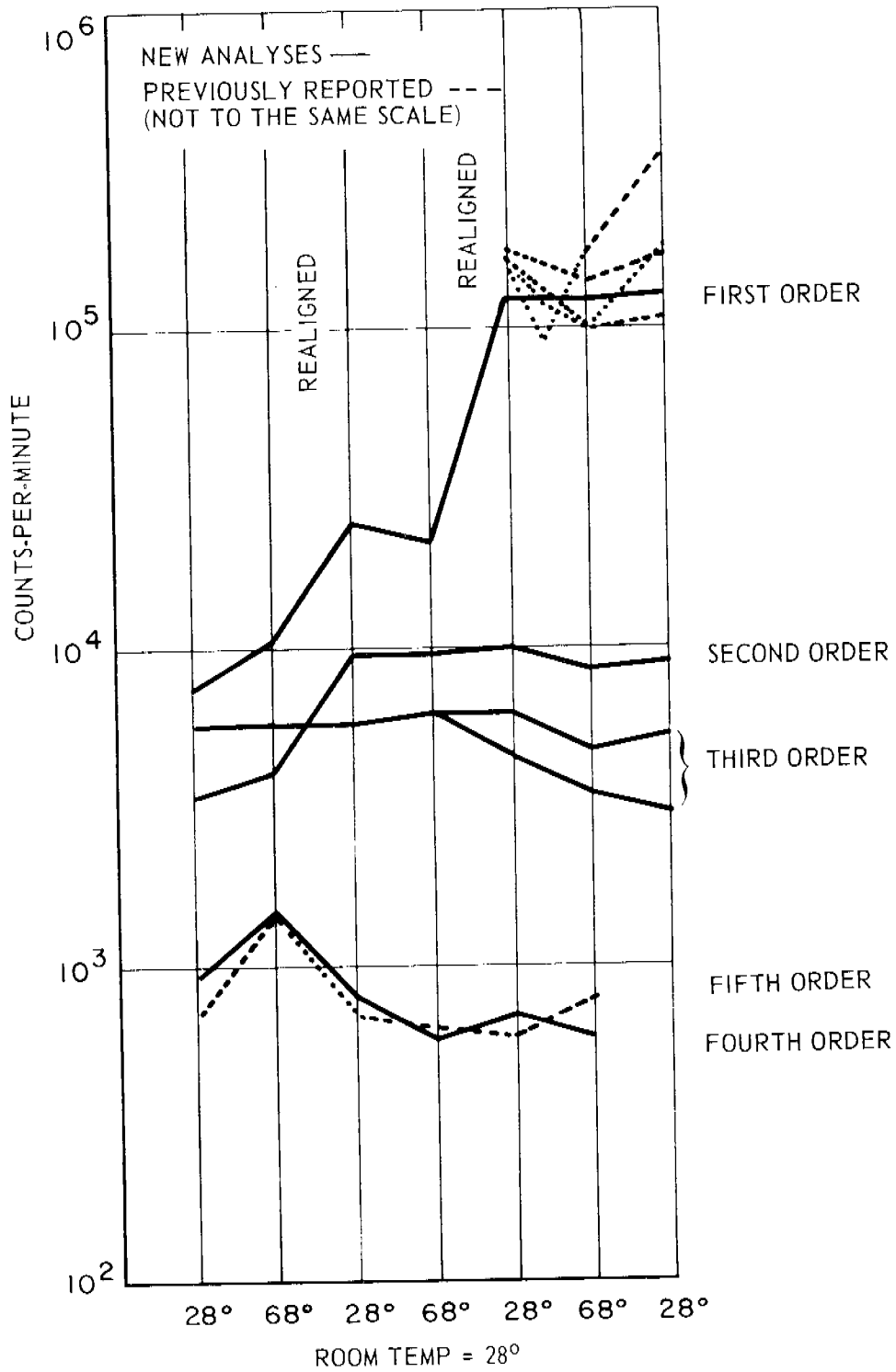


Figure 15. Barium Stearate X-Ray Diffraction Intensity vs. Temperature

extremely low values of conductance, stringent precautions had to be taken in the reference experiments which were designed to separate the various conductance processes in order to isolate the process of interest -- diffusion of barium ions across or through the polar sheets. The studies (see figure 16) showed that the temperature dependence of conductance, both DC and AC, in the barium stearate multilayer is marked over a short temperature range as the temperature is raised. Outside this transition region, the conductance appears to be independent of temperature. It is too early to be certain of the origin of these effects. There is a high probability that they are the result of a phase transition in the multi-layer which is not detectable by X-ray diffraction. A summary of barium stearate membranes tested is shown in table 1.

It was also found that in multilayer membranes which contained no barium ions, conductance phase transitions could not be detected. Figure 17 shows the dependence of barium content of the multilayer structure upon pH of the substrate upon which the stearic acid monolayer is spread. At high pH, the barium content is high and the X-ray diffraction curve shows the multilayer to be correspondingly compressed as a result of the strong coulombic attractions in the polar sheets. As the pH is lowered and the barium ion content drops, the long spacing of the multilayer increases as the compressive coulombic attractions decrease. At pH 5.5, there is no more barium in the multilayer, and one can observe the pattern characteristic of stearic acid. It was found (see figure 18) that there was no temperature dependence of the conductance of multilayers prepared at pH 5.5, indicating that an ionic atmosphere in the polar sheets is a necessary requirement for the occurrence of a conductance transition.

Measurements of the dielectric constant of barium stearate multilayers revealed that these systems are hydrated. The values reported in table 2 are for the system as it comes from the trough, along with a value for a strongly dehydrated multilayer. This latter value agrees quite well with previously published work. The temperature range where conductance anomalies were found, 28-32°C. However, these studies will be repeated using hydrated multilayers to determine the influence of water on the dependence of dielectric constant on temperature.

TABLE 1  
DESCRIPTION OF BARIUM STEARATE MEMBRANE  
MANUFACTURE AND FATE

Memb. Width	Substrate pH	Film Pressure	Memb. Support	Assembly Cement	Support Geometry	Membrane Resistance* (ohms)	Memb. Potential Theoretical/ Observed	Fate
72 dbi	7.0	30 d/cm	FeSt/Glass	"Miracle" Epoxy	round window	$3 \times 10^{10}$ (0.1M)	1.0	Conduct. transition observed
100 dbi	7.0	30 d/cm	FeSt/Glass	"Miracle" Epoxy	round window	$4.2 \times 10^7$ (0.02M)	0.15	Discarded
54 dbi	5.5	32	FeSt/Glass	"Miracle" Epoxy	round window	Shorted ( $10^4$ )	--	---
50 dbi	5.5	35	FeSt/Glass	"Miracle" Epoxy	round window	$1.5 \times 10^9$	1.0	No Transition
66 dbi	6.0	35	FeSt/Glass	"Miracle" Epoxy	round window	$1.3 \times 10^8$	2.35	Discard
50 dbi	6.0	34	FeSt/Glass	"Miracle" Epoxy	round window	$5.0 \times 10^7$ (0.1M)	1.0	No Conduct. transition observed
50 dbi	7.0	32	FeSt/Glass	"Miracle" Epoxy	round window	$2 \times 10^9$	1.0	Transition Observed
50 dbi	7.0	32	FeSt/Glass	Union Carbide Epoxy	round window	$0.88 \times 10^9$	2.3	Discarded
50 dbi	8.0	34	FeSt/Glass	"Miracle" Epoxy	round window	$1.1 \times 10^9$	1.0	Conduct. transition observed
50 dbi	8.0	34	FeSt/Glass	Union Carbide Epoxy	round window	$5 \times 10^7$	2.4	Discarded
110 dbi 45	7.5	32	FeSt/Glass	Union Carbide Epoxy	round window	$10^{12}$	Potential Unstable	Failed in 24 hr

\*(0.01M BaCl<sub>2</sub> electrolyte unless noted)

TABLE 1 (Cont'd)  
DESCRIPTION OF BARIUM STEARATE MEMBRANE  
MANUFACTURE AND FATE

Memb. Width	Substrate pH	Film Pressure	Memb. Support	Assembly Cement	Support Geometry	Membrane Resistance* (ohms)	Memb. Potential Theoretical/ Observed	Fate
100 dbi	8.0	32	Octadecyl-amine on quartz	Union Carbide Epoxy	small rectangular window	$2 \times 10^8$	---	Epoxy failed
100 dbi	8.0	35	Octadecyl-amine on quartz	Union Carbide Epoxy	small rectangular window	$7.5 \times 10^7$	1.5	Epoxy failed
85 dbi	8.0	35	Octadecyl-amine on quartz	Union Carbide Epoxy	small rectangular window			Alignment slipped in assembly
85 dbi	8.0	35	Octadecyl-amine on quartz	Union Carbide Epoxy	small rectangular window	$1.8 \times 10^7$	2.5	Discarded
100 dbi	8.0	35	Octadecyl-amine on quartz	Union Carbide Epoxy	small rectangular window	$3.3 \times 10^8$		

\*(0.01M BaCl<sub>2</sub> electrolyte unless noted)

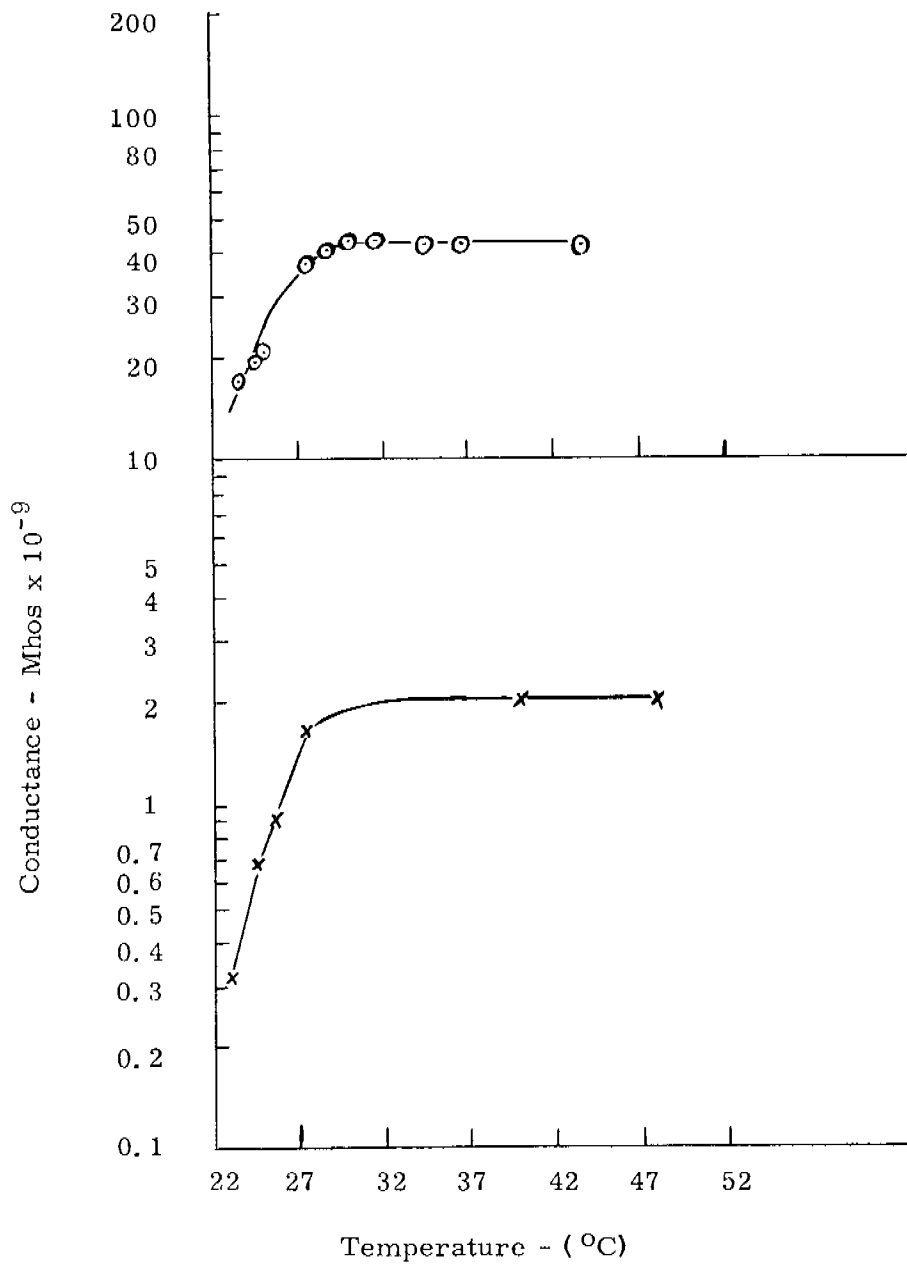


Figure 16. Conductance of Barium Stearate Multilayer Membranes vs. Temperature

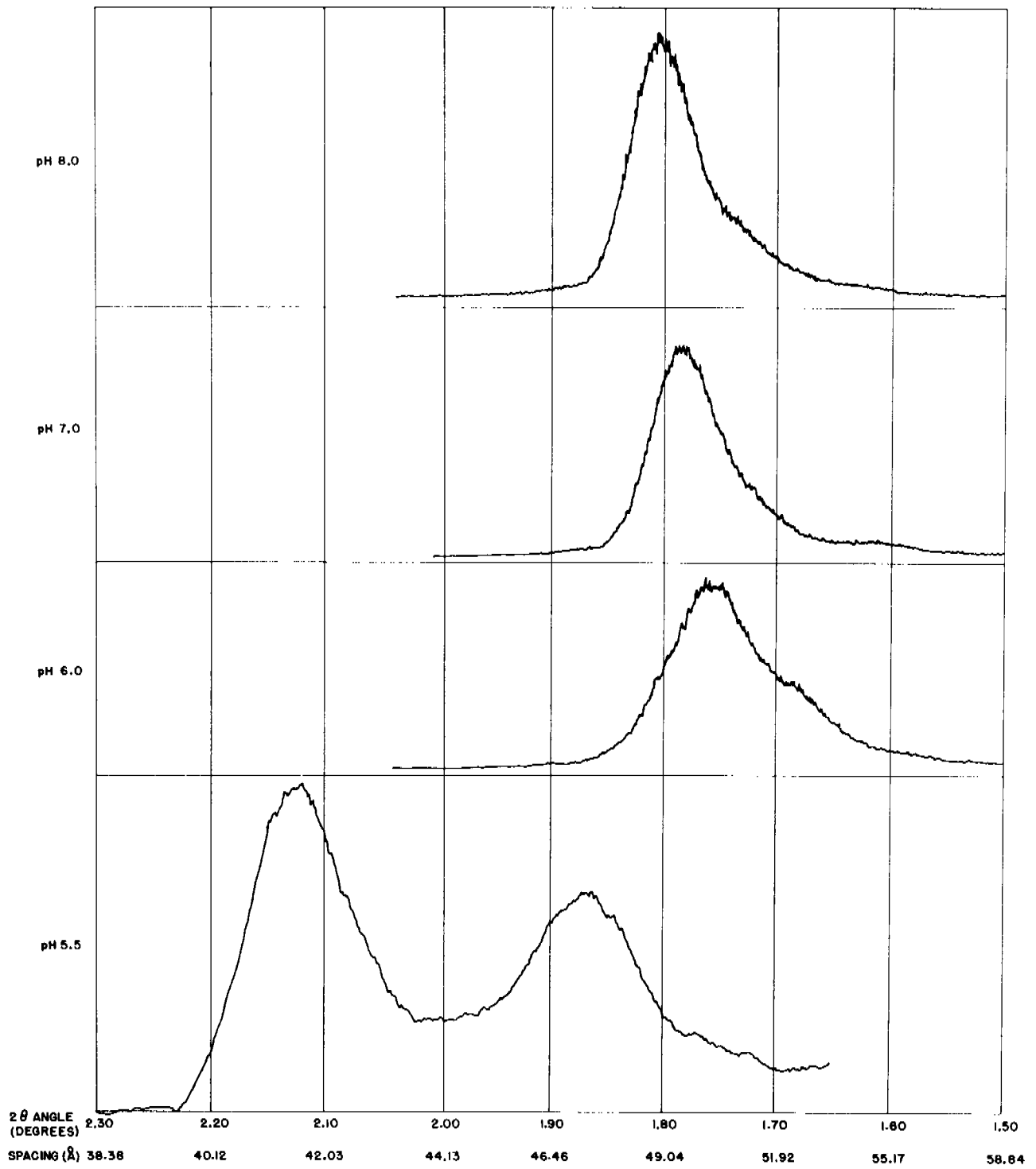


Figure 17. X-Ray Diffraction Intensity vs. pH

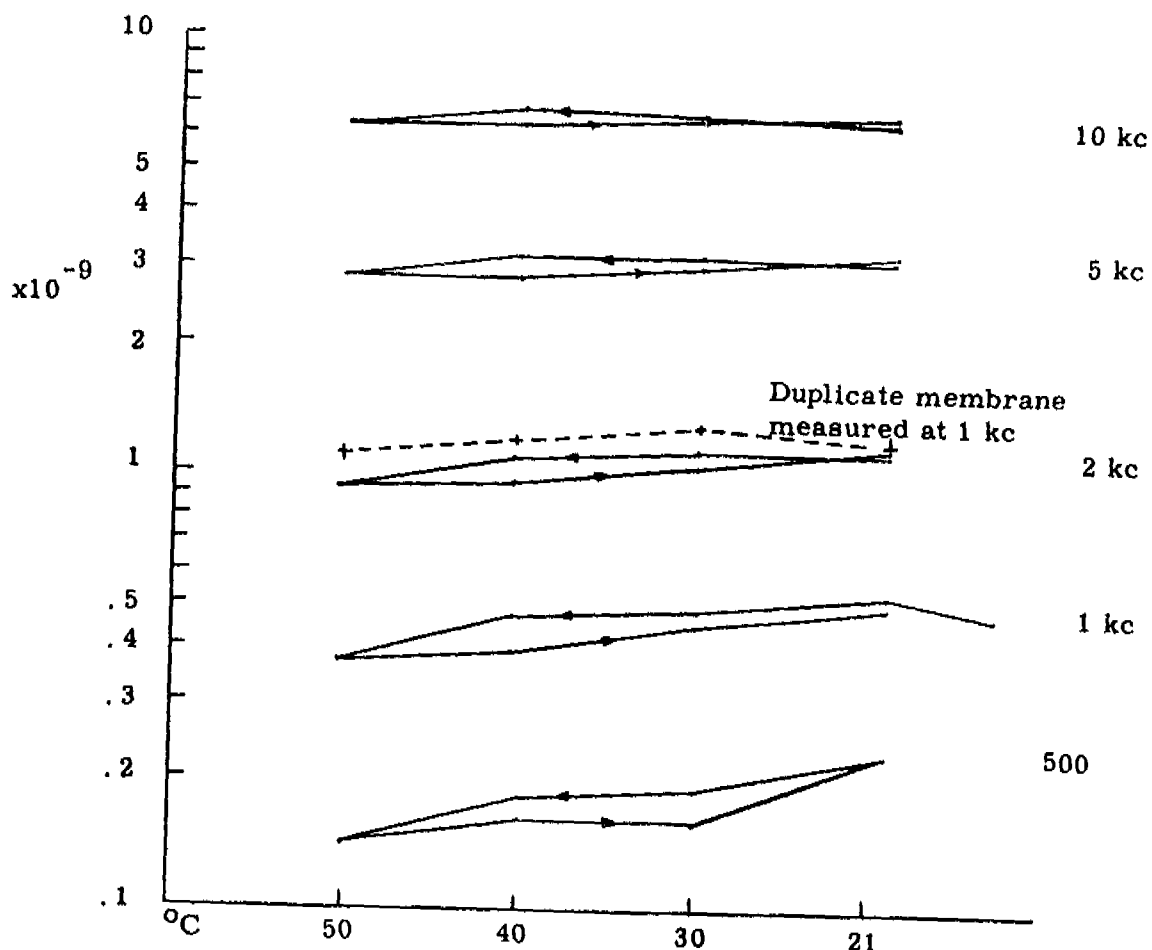


Figure 18. Conductivity of pH 5.5 Barium Stearate Multilayer Membranes vs. Temperature and Frequency

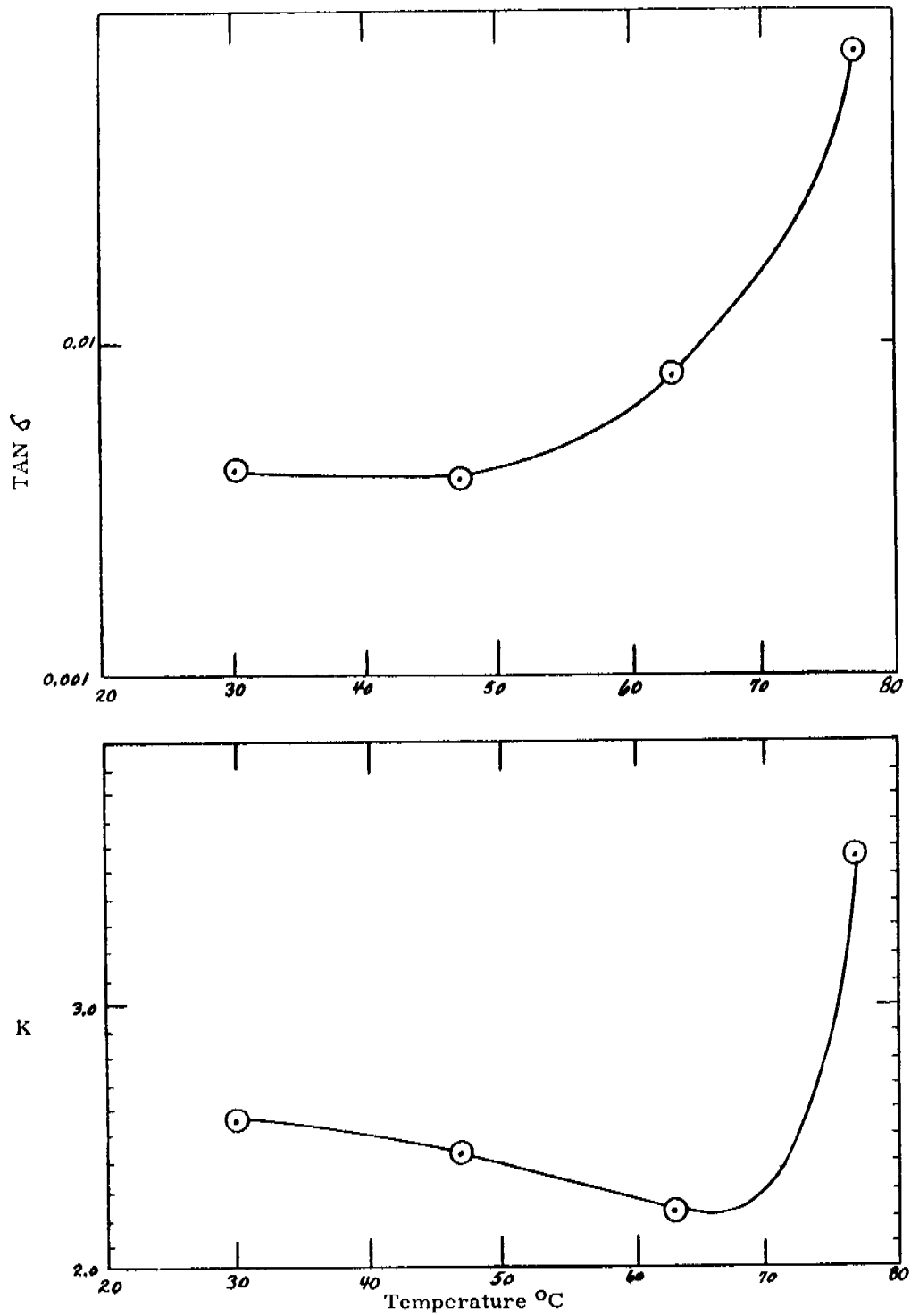


Figure 19. Dielectric Constant and Loss Factor of Barium Stearate Multilayer vs. Temperature

TABLE 2

DETERMINATIONS OF THE DIELECTRIC CONSTANT OF HYDRATED  
BARIUM STEARATE MULTILAYERS

---

Sample	
1	2.78
2	2.96
3	2.90
4	2.85
5	<u>2.87</u>
	Average
	2.87
	Standard Deviation
	0.03
6 Anhydrous	2.55*

---

\* Lit. value = 2.55

The nature of this "water of hydration" was investigated using Nuclear Magnetic Resonance. Wet, highly desiccated, and partially hydrated barium stearate were examined and the results appear in figure 20. It is clear that the water in the partially hydrated soap is bound, not free, as evidenced by the broad proton resonance peak. The free water in the wet sample is characterized by a sharp, narrow band, and the dry sample shows no proton peak at all.

### 3, 2            Soap and Polysoap Membranes

#### 3, 2, 1        Collodion - Potassium Oleate Membrane

Membranes consisting of several layers of collodion and potassium oleate were prepared and tested. The results of a study of concentration cell potentials and bi-ionic cell potentials are presented in table 3.

Since the 4-3-4 and the 4-4-4 collodion-potassium oleate membranes gave the highest bi-ionic potentials the preliminary investigations were confined to these systems. Since one of the main objectives of this program is to determine whether an order-disorder transition occurs within the lipid layer, a study was made of the effect of temperature on the bi-ionic membrane potential. An equimolar bi-ionic system (NaCl/KCl; 1 M) was then subjected to various temperatures, allowing sufficient time for membrane equilibration. To establish reproducibility, membranes were recycled over the temperature range from 0° to 50°C. Membranes were prepared by two different investigators using the established procedure with excellent reproducibility. The results of the temperature-cycle study are shown in figure 21. A maximum potential appears in the region between 8° and 15°C. The potential falls off at higher and lower temperatures. The maximum is not well defined on the high temperature side, but below 8°C, the membrane undergoes a deep-seated transition. This could be due to the formation of ice crystals, or to a change in the structure of the hydrated portions of the soap molecules in the micelles. A lipid transition at this low temperature does not seem to be justifiable on theoretical grounds (Kraft point).

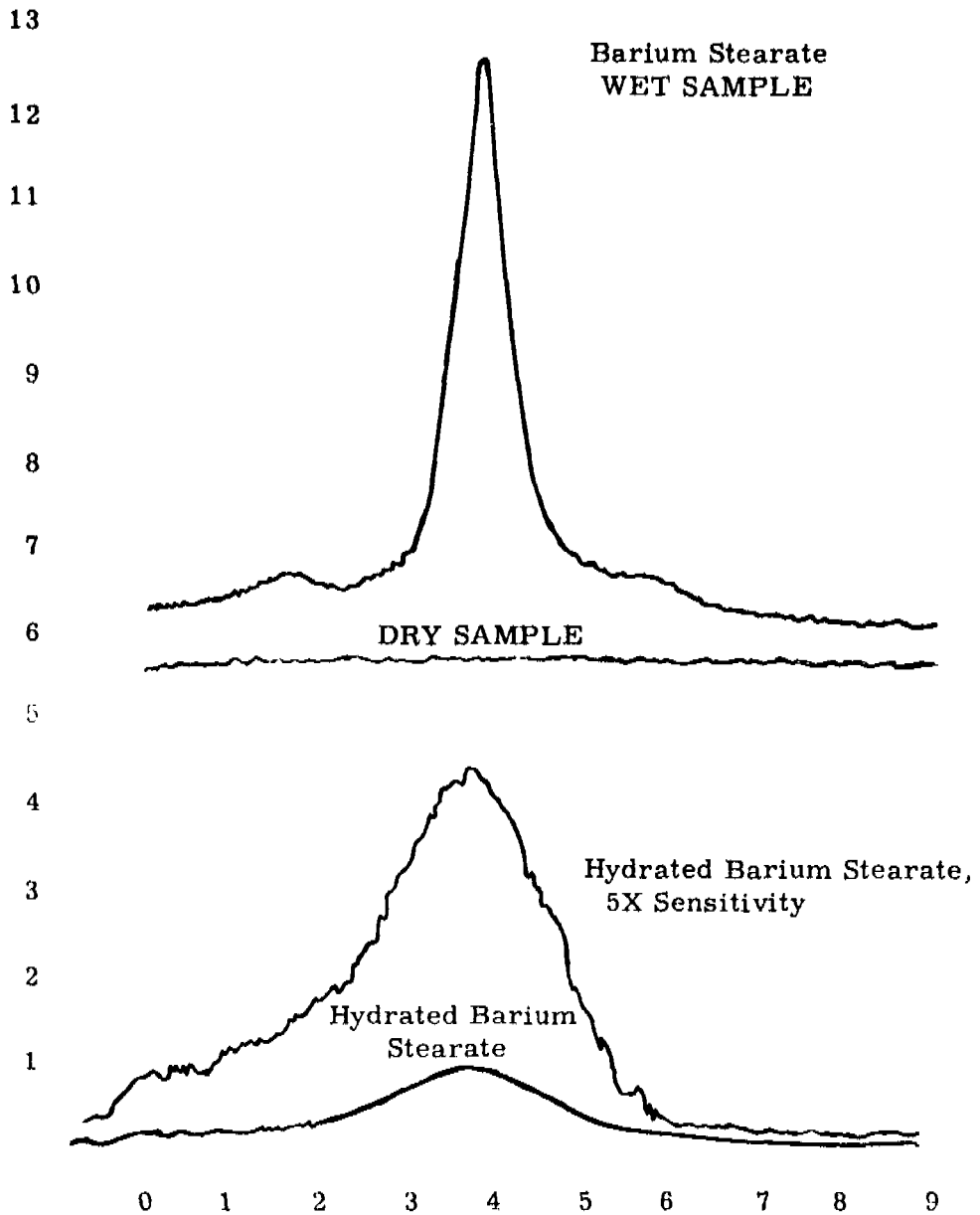


Figure 20. NMR Spectra of Wet, Hydrated, and Dehydrated Barium Stearate Powder. "Wet" Sample Dried One Hour Over Silica Gel at 1 mm Pressure to Remove Unbound Water

TABLE 3

## COLLODION-POTASSIUM OLEATE MEMBRANE POTENTIALS

Membrane	1 M KCl vs 1 M NaCl (mV)	0.1 M KCl vs 1 M KCl (mV)	Resistance ( $\times 10^5$ ohms)
4-4-4	29	57	4.6
4-3-4	26	58	5.4
3-3-3			
3-2-3	19	40	3.8
3-1-3	12	46	3.4
2-2-2			
2-1-2	6	42	3.0

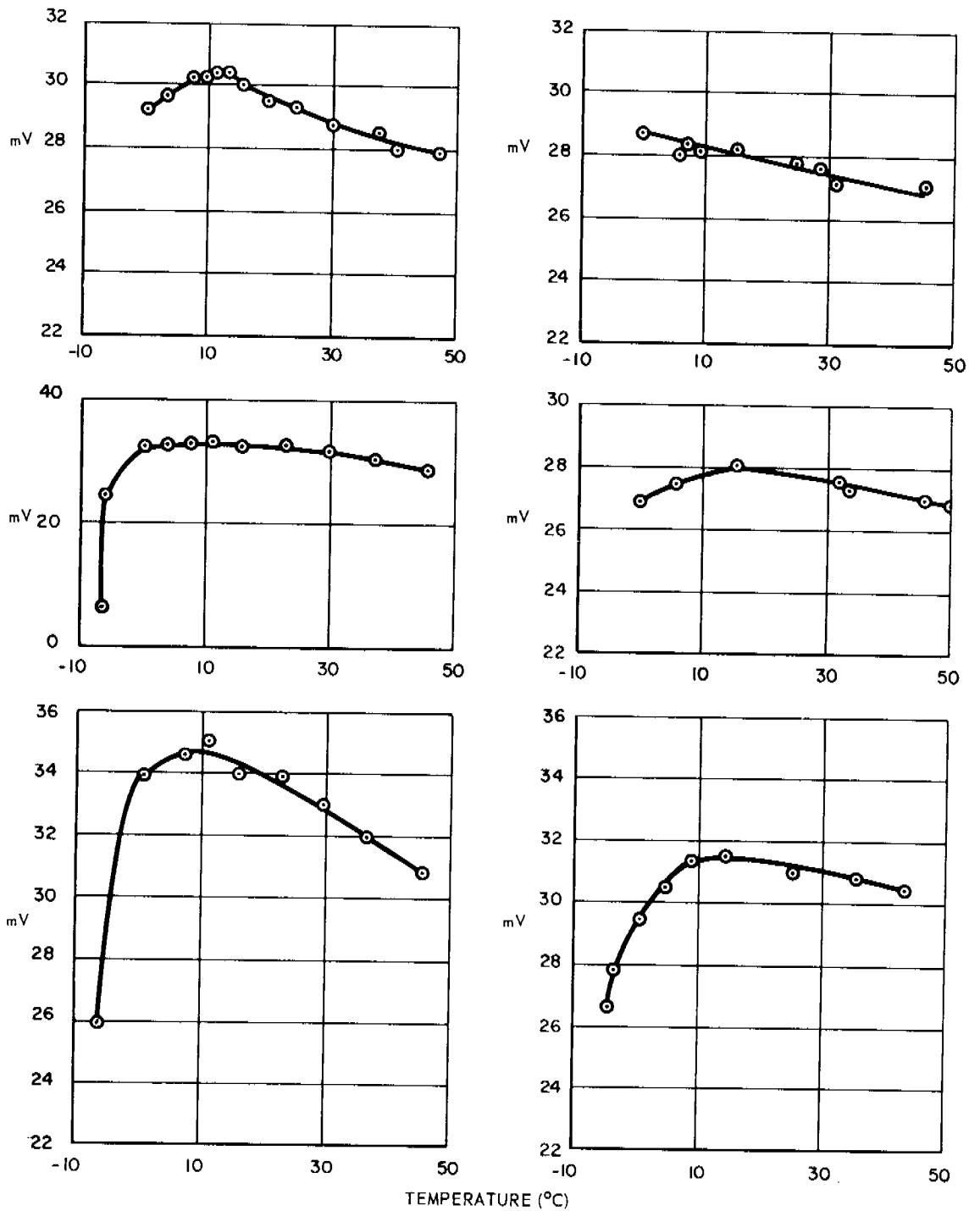


Figure 21. The Effect of Temperature on Membrane Bi-ionic Potential

The diffusion rates of sodium, potassium and lithium chloride solutions through the 4-3-4 collodion-potassium oleate membrane were determined conductometrically. The results of these studies are given in figure 22. The slope of the potassium chloride diffusion relationship is 1.46 times the value of the corresponding sodium chloride value. This is similar to the ratio of the diffusion rates of these two salts in water.

The results of a high temperature study of the bi-ionic potential of a 1M KCl/NaCl membrane system are shown in figure 23. When the membrane was subjected to temperatures higher than 90°C, the membrane deteriorated and exhibited a loss of sodium-potassium selectivity. The reversible behavior of the bi-ionic potential (figure 24) exists up to a maximum of 50°C.

#### Transport Numbers

It is assumed that an ideally permselective membrane has an activity-independent transport number equal to unity. The permselective behavior of this membrane is measured by the magnitude of the difference between the transport number of the cation and the transport number of the anion. For the determination of transport numbers, concentration ratios were kept equal to 2. The results of these experiments are presented in table 4. The average transport numbers of the sodium ions are typical of those of permselective ion-exchange membranes.<sup>2</sup> For higher concentration couples, the average transport number is much less than at lower concentrations.

The bi-ionic potentials of salt couples using a 4-4-4 collodion potassium oleate membrane are given in table 5. These are the potentials between 1,0 molar solutions of the chloride salts at a temperature of 24°C. The largest potential difference was obtained from the lithium-potassium couple in keeping with the hypothesis that the potassium ions diffuse at a greater rate than the lithium ions. The greater charge density of the smaller lithium ion firmly attracts a larger sphere of bound water

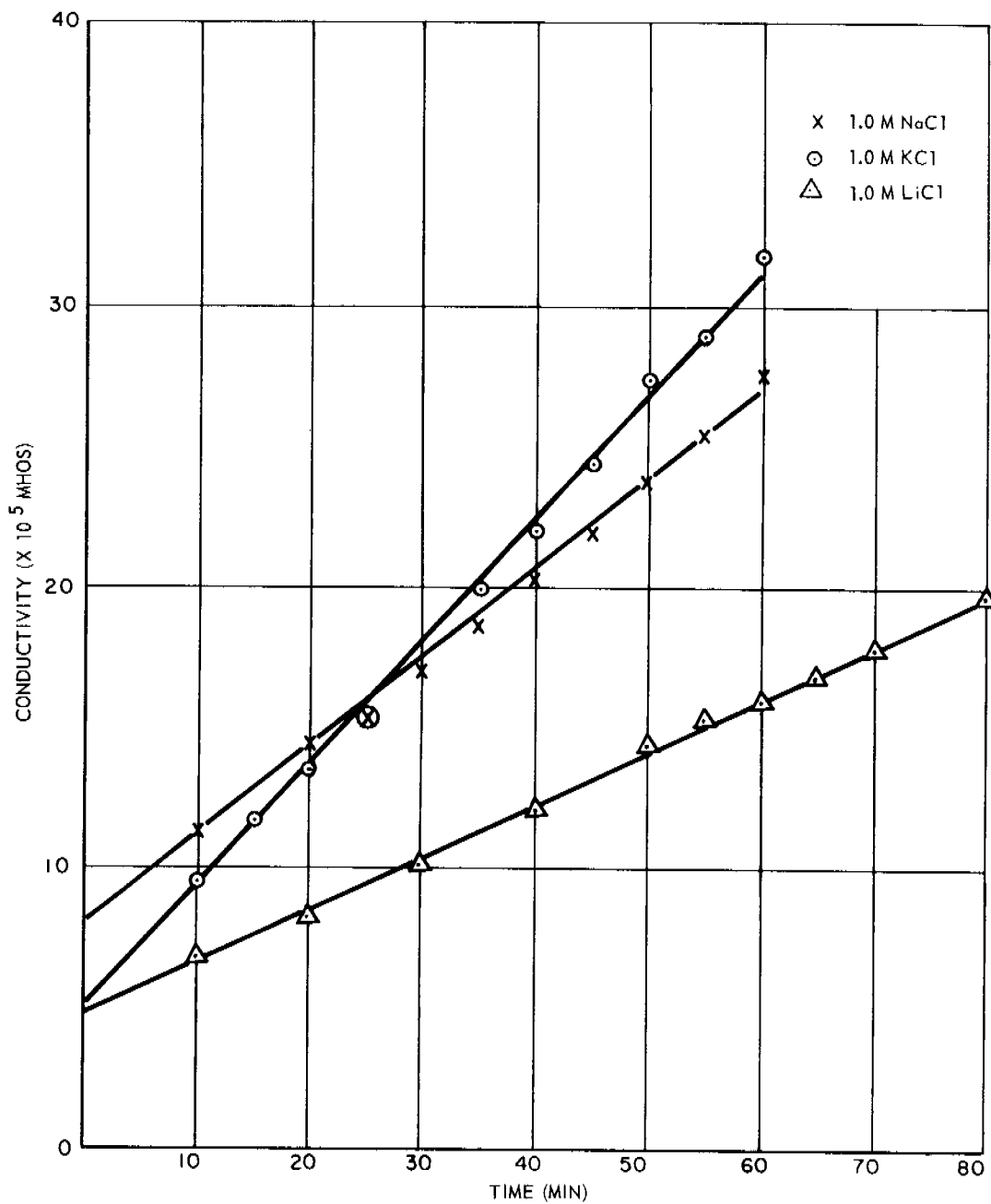


Figure 22. Electrolyte Diffusion Through a Collodion-Potassium Oleate Membrane

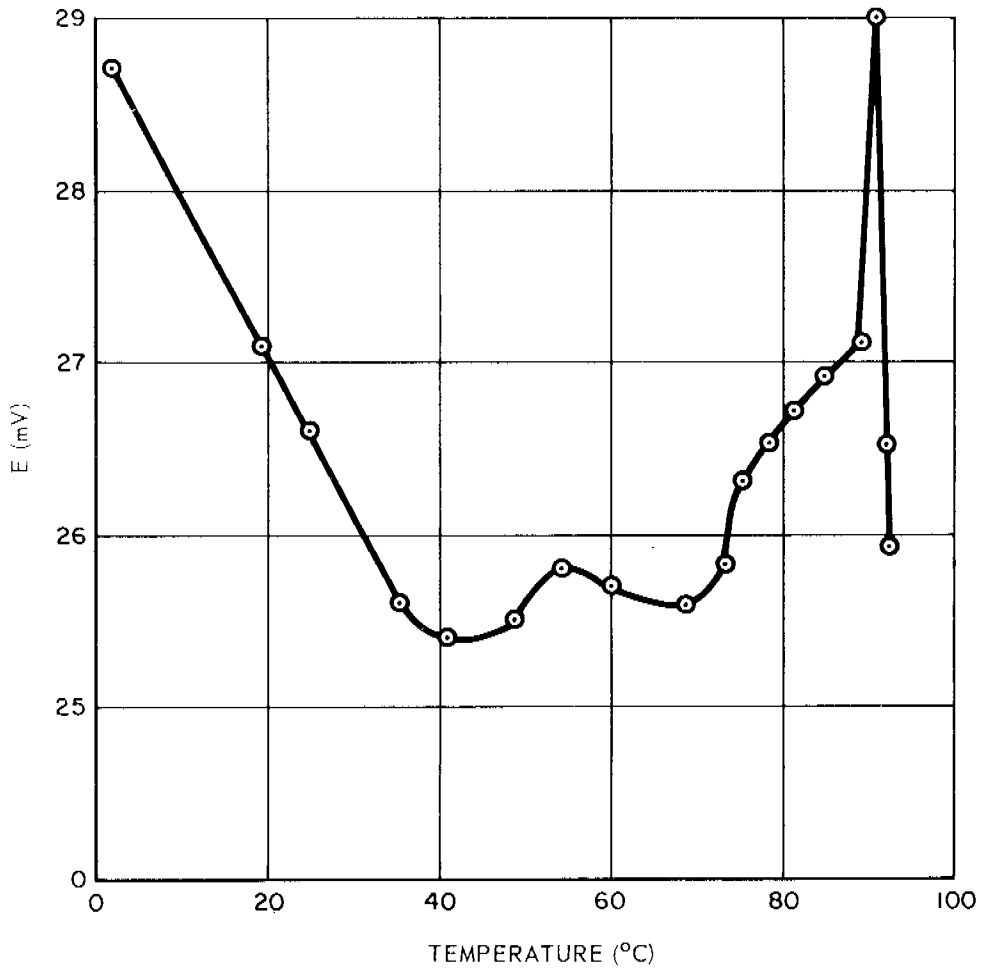


Figure 23. The Effect of Temperature on Membrane Bi-ionic Potential

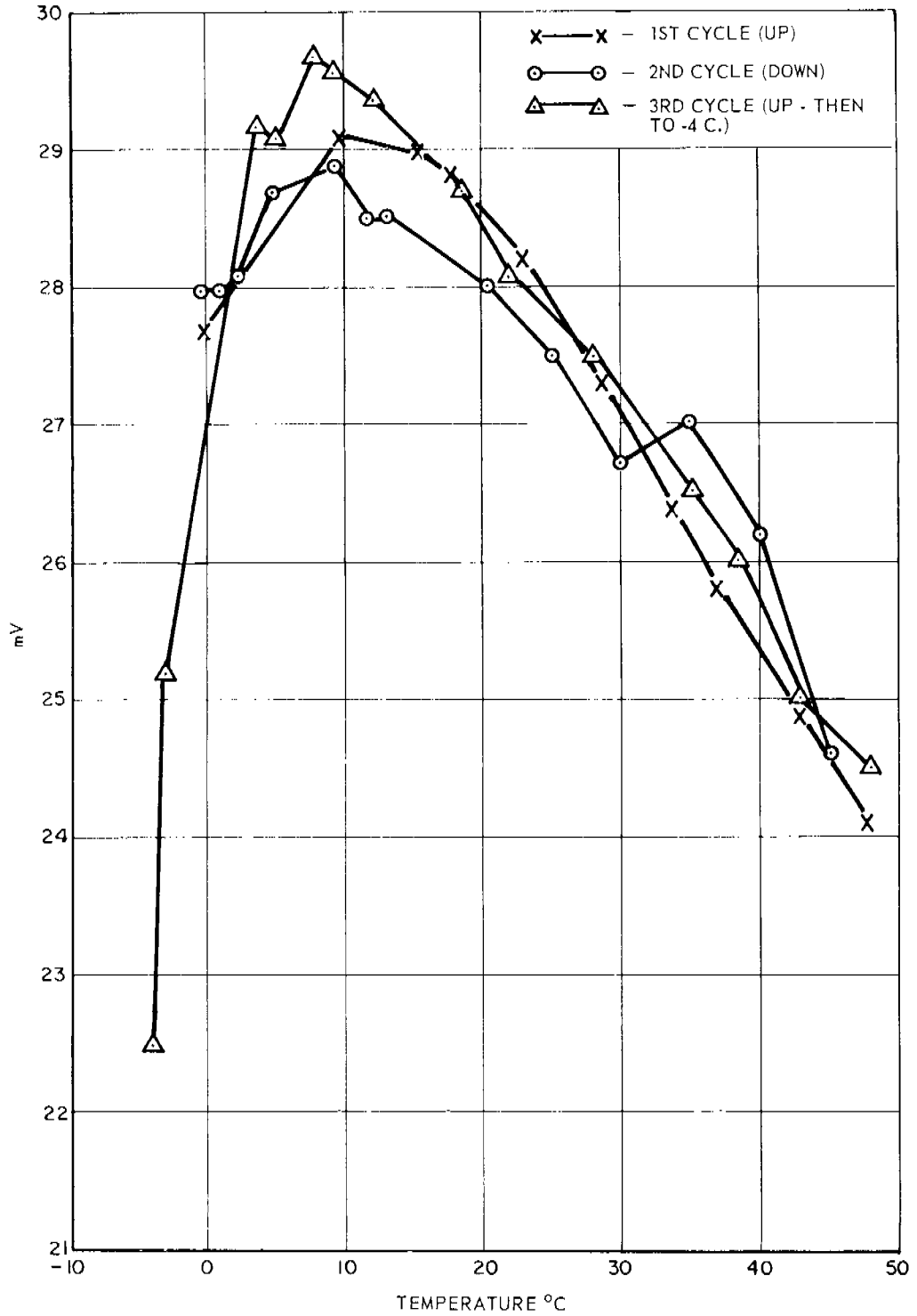


Figure 24. The Effect of Temperature on Membrane Bi-ionic Potential

TABLE 4

## CONCENTRATION CELL POTENTIALS

$C_1 - C_2$ KCL Solutions	E (Theoretical)	E (Experimental)	- $t_{x+}$
0.2 - 0.1	-16.11	-11.9	0.87
0.4 - 0.2		-15.5	
0.8 - 0.4	-15.89	-15.0	0.98
1.6 - 0.8		-13.0	
3.2 - 1.6		-13.8	
1.0 - 0.1		-48.0	0.954
NaCl Solutions			
0.2 - 0.1	-16.2	-13.3	0.91
0.4 - 0.2	-16.6	-14.5	0.94
0.8 - 0.4	-16.9	-14.2	0.92
1.6 - 0.8	-18.3	-13.8	0.89
3.2 - 1.6	-21.9	-12.0	0.89
1.0 - 0.1	-54.9	-51.0	0.78

molecules than does the larger potassium ion. This affects the effective "mass" of the hydrated ions as well as the viscous "drag" and the "ionic size." The bi-ionic potentials of two quaternary ammonium bromide systems are presented in table 6. It appears that the large hexadecylcetyl ammonium ion passes through the membrane quite readily in spite of its size. It is easy to explain this fact on the basis of the very low charge density of this ion without bothering to specify whether this is due to a "size", "drag", or "mass" effect.

TABLE 5

## TABULATED BI-IONIC POTENTIALS (0.5 MOLAR)

Salt Couple	E (mV)
	Observed
NR <sub>4</sub> Br/KBr	45
NR <sub>4</sub> Br/LiBr	55

\* (see discussion of results)

TABLE 6

## TABULATED BI-IONIC POTENTIALS (1 MOLAR)

Salt Couple	E* (mV)	E (mV)
	Theoretical	Observed
KCl/KCl	0.0	6
NaCl/LiCl	2.4	--
KCl/NaCl	4.8	28
KCl/LiCl	6.8	46
KCl/NH <sub>4</sub> Cl	0.0	15
NH <sub>4</sub> Cl/LiCl	6.8	50

## Matrix Free Soap Systems

The selective properties of a soap system in the absence of a collodion supporting structure were evaluated by study of a 0.1 molar sodium stearate gel. A hot soap solution was applied directly to the fritted glass of a "U" tube cell and allowed to gel. This soap gel system did exhibit a high  $K^+ / Na^+$  bi-ionic potential (approx. 28 mv); it was found to dissolve slowly in the electrolyte solutions. In a second experiment, a 0.1 molar sodium stearate gel was formed between two permeable (non-selective) dialysis membranes in an endeavor to prevent the outward diffusion of soap molecules. The effects of the salt concentration on the bi-ionic potentials of this "membrane" system are shown in figure 25.

## Collodion-Polysoap Membrane

Two polysoap membrane systems were prepared and tested. The first system consisted of three layers of collodion, three layers of dried 10 percent polysoap solution, and three layers of collodion. The other membrane was identical in all respects except that it was thinner (2-2-2). The 2-2-2 type of membrane gave much higher membrane potentials. These membranes showed a very high permselectivity for sodium, potassium and lithium ions (tables 7 and 8).

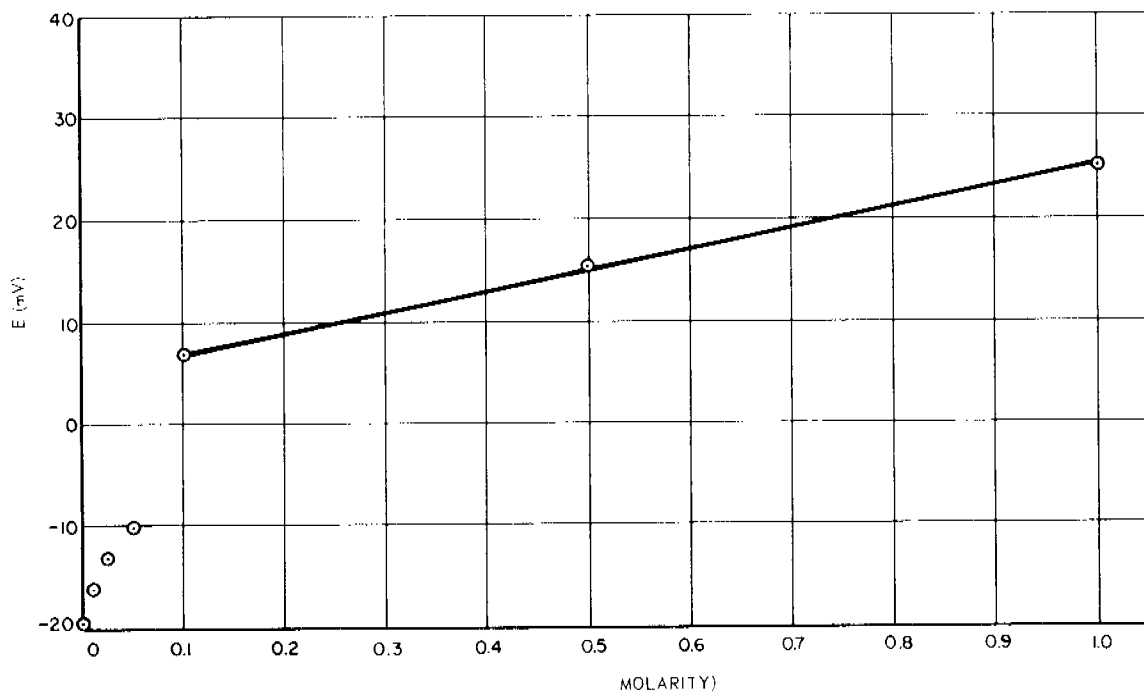


Figure 25. Bi-ionic Potential of 0.1 M Sodium Stearate Gel as a Function of Electrolyte Concentration

TABLE 7

## COLLODION-POLYSOAP MEMBRANE (3-3-3) POTENTIALS

Salt Couple (M)	E (mV)
1.0 M KCl vs 1.0 M KCl	4
0.1 M KCl vs 1.0 M KCl	27
1.0 M KCl vs 1.0 M NaCl	27
1.0 M KCl vs 1.0 M LiCl	52
1.0 M KCl vs 1.0 M NH <sub>4</sub> Cl	-8
1.0 M NH <sub>4</sub> Cl vs 1.0 M LiCl	58
0.1 NaCl vs 1.0 M NaCl	38

---

TABLE 8

## COLLODION-POLYSOAP MEMBRANE (2-2-2) POTENTIALS

Salt Couple (M)	E (mV)
0.1 M KCl vs 1.0 M KCl	37
1.0 M KCl vs 1.0 M NaCl	34

RESULTS

Table 9 - Diffusion Rates and BIP Values of non-selective collodion as a function of membrane thickness.

Number of Layers	dC <sub>NaCl</sub> /dt (umhos/min)	Temp. = 25.0°C		LM E	NaCl/KCl E*
		dC <sub>KCl</sub> /dt (umhos/min)			
2	5.94	3.22		3.0	0.7
4	.017	.042		3.7	1.4

Membrane casting solution - 50 ml (15% parlodion in 1:1 Methanol - ether) + 200 ml acetone

E\* = E - Electrode Asymmetry

Table 10 - Collodion diffusion rates and BIP's as a function of ether-acetone ratio.

Temp. = 25°C

Membrane Number	ml stock	ml ether	ml acetone	dC <sub>NaCl</sub> /dt (umhos/min)	dC <sub>KCl</sub> /dt	LM NaCl/KCl	
						E	E
1	5	0	10	.352	.174	3.3	1.0
2	5	4	6 *			3.6	1.3
3	5	6	4 *			6.8	4.5
4	5	10	0 *			8.0	5.7

Stock solution - 15% parlodion (1:1 ether - acetone solvent)  
 Membrane thickness - 3 layers cast (approx. 0.0003")

\* Extremely slow diffusion

Table 11 - Effect of Thickness on Diffusion through Glycerol Graded Collodion.

Membrane Thickness (layers)	$dC_{NaCl}/dt$ (umhos/min)	$dC_{KCl}/dt$ (umhos/min)	1M NaCl/KCl E*
2	3.47	2.61	2.1
4	.125	.172	1.1
6	0.00	0.00	2.9

Membrane casting solution - 3% parlodion and 0.2% glycerol in methanol

Table 12 - Permselective Characteristics (transport numbers) of the Collodion used in the Preparation of PS 3-1-1-1 and PS 3-1-2-1 Membranes.

Temp. = 25.0°C

Expt. Type	Cell	(umhos/min)	E	E*	$E_0$	t+	t-	Collodion layers
diff.	NaCl/H <sub>2</sub> O	.393	--	--	--	--	--	one
diff.	KCl/H <sub>2</sub> O	.142	--	--	--	--	--	one
BIP	NaCl/KCl .01M	---	3.4	1.1	--	--	--	one
BIP	NaCl/KCl .1M	---	10.9	8.6	--	--	--	one
BIP	NaCl/KCl 1.0M	---	9.1	6.8	--	--	--	one
Conc.	KCl/KCl .01M - .1M	---	17.5	15.2	55.2	.538	.462	one
Conc.	KCl/KCl 0.1M - 1.0M	---	4.2	1.9	53.1	.518	.482	one
Conc.	NaCl/NaCl .01M - .1M	---	0.8	1.5	55.3	.514	.486	one
Conc.	NaCl/NaCl .1M - 1.0	---	2.2	0.1	54.8	.501	.499	one
BIP	NaCl/KCl 1M	---	8.9	6.6	----	---	---	two

Membrane casting solution - 7% parlodion in Methanol

Table 13 - Permselective Properties of a PS 3-1-1-1 Membrane Immediately after Casting and Air Drying.

Temp. = 25.0°C

Expt. No.	Cell	E	E*	E <sub>0</sub>	$\bar{t}_+$	$\bar{t}_-$
1	Ko/NaO 0.1M - 0.1M	36.0	33.7	--	--	--
2	Ko/Ko 0.1M - 0.05M	0.0	-2.3	--	--	--
3	KCl/KCl 0.1M - 0.05M	7.0	4.7	16.0	0.647	0.353
4	NaCl/NaCl .1M - .01M	32.0	29.7	55.4	0.768	0.232
5	NaCl/NaCl 1.0M - .1M	35.0	32.7	54.8	0.798	0.202
6	NaCl/NaCl 1.0M - 0.5M	4.6	2.3	17.0	0.568	0.432

Polysoap casting solution - 10% PS 3 in methanol

Collodion casting solution - 7% parlodion in methanol

KO = potassium oleate, NaO = sodium oleate

Table 14 - Permselective Properties of a PS 3-1-1-1 Membrane after Drying for 24 hours.

Temp. = 24.5°C

\* See Discussion

Extp. Type	Cell	E	E*	E <sub>0</sub>	$\bar{t}_+$	$\bar{t}_-$	Notes
BIP	NaCl/KCl 1M	31.9	29.6	*	--	--	
Conc	KCl/KCl 1M - .01M	78	75.7	108	0.850	0.150	
Conc	NaCl/NaCl 1M - .01M	68	65.7	110	0.799	0.201	
Conc	KCl/KCl .1M - .01M	35	32.7	55.1	0.818	0.182	
Conc	NaCl/NaCl .1M - .01M	23.1	20.8	55.3	0.688	0.312	
BIP	NaCl/KCl .01M	19.1	16.8	*	--	--	
BIP	NaCl/KCl 0.1M	26.1	23.8	*	--	--	
BIP	NaCl/KCl 1M - 1M	31.0	28.7	*	--	--	
diff.	KCl/H <sub>2</sub> O 1M	--	---	---	--	--	

Table 15- Permselective Properties of a PS 3-1-1-1  
Membrane after Air Drying for One Week.

Temp. = 25.0°C

Expt. Type	Cell	E	E*	E <sub>o</sub>	E <sub>+</sub>	E <sub>-</sub>	BIP E <sub>o</sub> (a)	BIP E <sub>o</sub> (b)	BIP E <sub>o</sub> (c)	$\sum E_o$
Conc	NaCl/NaCl 1M - .1M	54.0	51.7	54.9	0.971	0.029				
Conc	KCl/KCl 1M-0.1M	43.0	40.7	52.9	0.886	0.114				
BIP	NaCl/KCl 1M	25.1	22.8				5.61	4.38	5.86	15.9
Conc	NaO .1M-.01M	17	14.7	No available activity data for oleates						
Conc	KO .1M - .01M	20.5	18.2							
BIP	NaO/KO 1M	33	30.7							
BIP	KCl/KO 0.1M-0.1M	-3.0	-5.3							
BIP	NaCl/Ko 0.1M-0.1M	15.9	13.6							
BIP	NaCl/KCl .1M-.1M	29.4	27.1							
BIP	NaCl/NaO 0.1M-0.1M	-3.6	-5.9							

(a) Calculated from Lewis and Sargent Equation

(b) Calculated from Transport Numbers

(c) Calculated from diffusion coefficients

(See Discussion)

Table 16 - membrane Transport Numbers for various (non-polymeric) oleate systems

Temp. = 25.0°C

Membrane	KCl/KCl Cell	E	E*	E <sub>0</sub>	$\bar{t}_+$	$\bar{t}_-$
3-2-3	.1M-1M	40	39	52.9	.869	.131
3-1-3	" "	46	44	52.9	.916	.084
2-1-2	" "	42	40	52.9	.879	.121

Table 17 - Membrane Transport Numbers; PS 3-4-4-4 Membrane.

Temp. = 25.0°C

KCl/KCl concns.	E*	E <sub>0</sub>	$\bar{t}_+$	$\bar{t}_-$
.2M-.1M	11.9	16.0	.872	.128
.4M-.2M	15.5	15.9	.987	.013
.8M-.4M	15.0	15.85	.973	.027
1.6M-.8M	13.0	16.2	.901	.099
3.2M-1.6M	13.8	17.3	.899	.101
1.0M-0.1M	48	52.9	.954	.046

NaCl/NaCl concns.	E*	E <sub>0</sub>	$\bar{t}_+$	$\bar{t}_-$
.2M-.1M	13.3	16.4	.906	.094
.4M-.2M	14.5	11.1	---	---
.8M-.4M	14.2	16.6	.928	.072
1.6M-.8M	13.8	11.3	---	---
3.2M-1.6M	12.0	19.9	.801	.199
1.0M-.1M	51.0	54.9	.964	.036

Table 18 - Anion Permselectivity of a PS 3-1-2-1 Membrane and Calculated, BIP's

Temp. = 25.0°C

Cell	E*	BIP E <sub>0</sub> (a)	BIP E <sub>0</sub> (b)	BIP E <sub>0</sub> (c)	$\bar{t}_-$	$\sum E_0$
KBr/KI 1M	-8.6	0.18	1.54	2.84	.255Br .259I	4.56
KBr/KI .1M	-23.5	0.41	1.30	0.59	.395Br .413I	2.30
KBr/KCl 1M	-7.75	0.36	0.886	1.95	.255Br .252Cl	2.20
KBr/KCl .1M	-21.1	0.18	1.12	0.47	.395Br .379Cl	1.77
KI/KCl 1M	-7.75	0.12	2.42	4.66	.259I .252Cl	7.20
KI/KCl .1M	- 21.7	0.18	2.42	1.006	.413I .379Cl	3.60

(a) Calculated from Lewis and Sargent Equation

(b) Calculated from Transport Numbers

(c) Calculated from diffusion coefficients

See Discussion

Table 19 - Cation Permselectivity (various anions)  
PS 3-1-2-1 Membrane and Calculated BIP's

Temp. = 25.0°C

Cell	E <sub>0</sub>	E	E*	$\bar{t}_+$	$\bar{t}_-$
KBr/KBr 1M-.1M	53.4	28.4	26.1	0.745	0.255
KBr/KBr .1M-.01M	55.1	13.9	11.6	0.605	0.395
KCl/KCl 1M-0.1M	52.9	28.5	26.2	0.748	0.252
KCl/KCl 0.1M-0.01M	55.0	15.6	13.3	0.621	0.379
KI/KI 1M-.1M	54.4	28.5	26.2	0.741	0.259
KI/KI 0.1M-0.01M	55.3	11.9	9.6	0.587	0.413

Table 20 - Further tests of the Pauling Theory of  
Molecular Anesthesia - Effect of Argon  
and Nitrogen Saturation (one atmosphere)  
on BIP.

Temp. °C	KCl/NaCl 1M E	Gas
22.0	24.1	-----
22.3	23.9	Argon (1 atmosphere)
22.4	24.0	Nitrogen (1 atmosphere)
20.5	25.1	-----
24.9	24.7	-----
24.7	24.45	-----
22.6	24.2	Nitrogen (1 atmosphere)

## 4. DISCUSSION

### 4.1 Multilayer Crystals

The experimental apparatus was constructed during the 1st Quarter. The apparatus was improved during the 2nd Quarter and procedures for preparing force-area curves on surface films and for depositing multilayer structures were devised.

During the third Quarter work on surface-chemical characterizations of various lipid materials, multilayer deposition, studies and assembly of concentration cells and their use in electro-chemical measurements was performed.

Barium stearate multilayer structures were successfully formed at surface pressures from 25 to 35 dynes/cm at moderate dipping speeds (slower than 5 cm/min). X-ray diffraction intensities could be correlated with barium content which is dependent on substrate pH. Inclusion of  $10^{-6}$  M copper ion in the substrate films appears to permit deposition with no visual defects at fast dipping speeds.

It appeared that a multilayer structure exhibited a reversible change in peak intensity with temperature when heated to temperatures lower than the melting point of stearic acid. A time-dependent recrystallization was also observed in this system when heated to slightly above the melting point of stearic acid. Powdered barium stearate was characterized by an X-ray diffraction peak corresponding to the 49.3 Å double-layer spacing, but the peak intensity of this peak was much lower than that of the multilayer, indicating a less ordered structure. X-ray diffraction peak intensity of the recrystallized multilayer suggested a disorder of the 49.3 Å interplanar spacing comparable to that of the polycrystalline powdered material. These facts suggest that a partial, reversible phase change may occur below the melting temperature of stearic acid in a stearic acid-barium stearate multilayer, and that a recrystallization to a polycrystalline material occurs above the melting temperature of stearic acid. Further study was expected to show the effect of barium content (as determined by substrate pH at the time of multilayer deposition), and the quantitative effect of temperatures near the melting point of stearic acid.

Irradiation in an X-ray beam of high intensity for an extended time does disturb the crystal regularity, and causes visual darkening of the material.

A barium stearate multilayer membrane in a concentration cell developed a potential close to that predicted by theory, indicating true cation selectivity. However, in the presence of a high concentration of electrolyte, the membrane was no longer reversible, i.e., reversing solutions in cell chambers resulted in an asymmetric potential.

Cerotic acid, 26 carbons long, was found to have a force-area curve similar to that of stearic acid, but film collapse did not occur up to 55 dynes/cm. The film appeared quite viscous and this interfered with successful transfer of the film to glass slides. Probably docosanoic acid ( $C_{22}$ ) or linocerinic acid ( $C_{24}$ ) can be used as a longer chain material than stearic acid for preparation of multilayer structures. These longer chain fatty acids can be expected to form more ordered structures.

A barium lecithinate film could not be transferred to a slide, but a barium cephalinate film was deposited. Conditions will be sought which will permit a multilayered cephalinate structure to be constructed for analysis. If the alkali cephalinates are sufficiently insoluble in water the alkali cephalinate multilayer system may exhibit ion specificity comparable to that obtained from the insoluble to the film for reproducible deposition. The surface pressure of the film must remain constant during deposition if the surface density of the film being deposited is to be identical to that of the film on the water. It is apparent that a knowledge of the solid state characteristics of the deposited film depends on a thorough knowledge of the structure of the monolayer at the air/water interface. The two critical parameters here are the surface density or what may be more familiar, the area per molecule, and the orientation of each molecule which may be estimated by the surface dipole moment determined through measurements of the surface potential.

In order to study the mobility of the various cations in the synthetic crystals, salts of the ionic lipids must be deposited. This may be accomplished by spreading the lipids

on a solution containing the cations required. Salt formation may be expected to occur under these conditions, thereby producing the desired surface species. It is therefore necessary to thoroughly characterize each of these ionic lipid salts so that the surface state appropriate for deposition may be obtained. It is clear that before any solid state measurements can be made, precise surface chemical studies must be done.

#### 4.2 Soap and Polysoap Membranes

Because of the experimental difficulties encountered in the use of the barium stearate multilayer system as a model biological membrane a series of additional approaches had been initiated. These approaches were designed to test the hypothesis that a temperature dependent phase transition will be observed in the model membrane system, and whether or not this transition is a reversible one occurring in the lipid or "soft ice" regions of the model.

Sodium and potassium ion selectivity were studied as a function of temperature. Membrane bionic potentials were measured between equimolar sodium and potassium chloride solutions. In addition, the salt diffusion rates through these membranes was at constant temperature. A truly reversible transition is signalled by superimposable data from subsequent temperature cycles.

##### 4.2.1 Polysoaps

Polysoaps are polymers which are built up of soaplike structural units. Because of their high molecular weights and bulkiness, it was assumed that they could be readily imbedded in a matrix and reduce the problem of soap diffusing out of the matrix. Ideally, the matrix and the soap are chemically bonded into one unit. The preparation of the polysoap gave a product that had an "undesirable" color. This was due to the fact that the polysoaps were prepared in nitrobenzene rather than in nitropropane, which is claimed to give a product of lighter color<sup>2</sup>.

When the polysoap is wet, it is readily soluble in water. The physical characteristics of the polysoap resemble

those of an organic polymer. These polysoaps are elastic and sticky. When the polysoaps are dried the product is resinous and brittle. This dried form may be redissolved in boiling water.

The first attempts to prepare a polysoap membrane failed because the polysoap was insoluble in the acetone ether solvent of the collodion solution. The aqueous method produced membranes having very good physical properties. Membranes prepared in this manner were flexible and strong and resisted delamination.

#### 4.2.2 Transport Numbers

The method of obtaining cation transport numbers in the membrane matrix closely follows the derivation and justification presented by Clarke et al<sup>5</sup>. For the average transport number,  $\bar{t}_+$ , of an ion in the membrane phase,

$$\bar{t}_+ = E + E_o / 2E_o = E / 2E_o + 0.5,$$

$E_o$  is the theoretical potential of a concentration cell based on the two electrolyte activities.

$$E_o = RT/F \ln a_1/a_2$$

$E$  is the observed potential. If the difference between the concentrations of the aqueous solutions equilibrated with the membrane is small, only a small error is introduced by assuming that  $t_+$  is linear in  $\ln a^5$ .

#### 4.2.3 Junction Potentials

The  $E^*$  values in table 3 are from the Lewis and Sargent equation<sup>6</sup> and are the potentials to be expected in the absence of a membrane. This relationship is simply

$$E_L = RT/F \ln U_+ + U_-/U_+' + U_-' = RT/F \ln \Lambda / \Lambda' ,$$

where  $\Lambda$  and  $\Lambda$  are the equivalent conductances of two univalent electrolytes having an ion in common and are at the same concentration. The  $E_L$  values are essentially liquid junction potentials.

#### 4.2.4 Nature of the Reversible Transition

The transport numbers (in the membrane phase) of KCl and NaCl solutions were determined by the method of Medalia et al<sup>2</sup>. The close approach of these values to the theoretical ideal of unity suggests that these membrane systems are high permselective.

High selectivity is similarly suggested by the magnitude of the difference between the observed K/Na bi-ionic potentials and the predicted liquid-junction potential.

The low temperature maximum of the bi-ionic potential suggests the possibility of hydrate or ice formation in the electrolyte and/or membrane phase. This could be tested by using nonaqueous salt solutions in solvents of a much lower freezing point (e.g., dimethylformamide and dimethylsulfoxide).

The electrolyte diffusion studies have shown that the transmembrane diffusion rates of potassium and sodium are in the same ratio as those measured conductometrically in aqueous solution. This result indicates that only the magnitude of the diffusion rates may be affected by passage through the membrane but not the ratio of the two rates. This result indicates that only the magnitude of the diffusion rates may be affected by passage through the membrane but not the ratio of the two rates. This last point also holds for pure collodion membranes of the proper "pore size."

The soap gel studies appear to support the hypothesis that the K/Na specificity resides in the soap structure rather than in the collodion matrix.

#### 4.2.5 Permselectivity and "Pore" Size

A question arose concerning the role that the collodion supporting matrix plays in the total permselectivity of the laminated collodion-polysoap structure. Membranes made by

dissolving parlodion in methanol-ether-acetone, methanol-ether or pure methanol exhibit very low BIP's (Table 9, Table 10, Table 11). Alcohol acts as a swelling agent to produce very porous collodion membranes while high concentrations of ether in the casting solution produce very dense, non-porous membranes.

As shown in Table 9, additional layers of collodion do not cause a significant increase in the observed BIP's. There is, however, a marked decrease in the rate of salt transfer through the membrane. The effect that ether has on the porosity of the cast collodion membrane is also demonstrated by the gradually rising BIP seen in Table 10. The BIP rises as the concentration of ether is increased at constant collodion concentration and membrane thickness. This dramatic tightening of the collodion structure is emphasized by the extremely low rates of salt transfer through membranes cast from collodion solutions containing ether.

Very porous, homogeneous and mechanically strong membranes may be prepared by incorporating a non-volatile liquid in the casting solution. Solid substances cannot be used because crystallization occurs as the volatile solvent(s) evaporate. Glycerol graded collodion exhibits a very small degree of cation specificity and very large salt transfer rate, as shown in Table 11.

Fortuitously, parlodion is very soluble in the swelling solvent, methanol. Very porous, non-selective membranes may be prepared from casting solutions (7 - 10%) in this solvent. The collodion layers produced in this manner exhibit large  $dC/dt$  values and are quite porous. The ratio of the NaCl and KCl diffusion rates is close to the value determined in water (approx. 1.5). The various BIP's are very low and the membrane transport numbers derived from concentration cell measurements are very close to the 0.5 characteristic of an ideally non-selective membrane.

The fact that the collodion BIP's were polarized positively on the NaCl side of the couple indicates that a very slight cation specificity exists.

The permselective properties of a PS 3-1-1-1 membrane determined immediately after casting and drying are not as large as those exhibited by the same membrane dried for longer periods.  $\bar{t}_+$  values (Table 13) determined immediately after casting are smaller than those obtained after drying for longer periods (Table 14 and Table 15). The cation selectivity of a PS 3-1-1-1 membrane dried for approximately one week (Table 15) approaches very closely the behavior of an ideally permselective membrane. This solvent-free membrane must be handled with care because it cracks easily. This behavior closely parallels the change in properties observed when a methanol solution of polysoap is allowed to evaporate to dryness on a steam bath. A resinous gel is formed which converts to a very brittle porous solid upon further drying. The dry form may be readily ground to a fine dust.

The  $E_O$  values in Tables 13 and 14 were obtained from the expression for the potential of a concentration cell with transference using the appropriate activities.

$$E_O = \frac{RT}{F} \ln \frac{a_2}{a_1} = 59.1 \ln \frac{a_2}{a_1} \quad (25^\circ\text{C})$$

Activity coefficients, as well as several other electrochemical parameters, were obtained from the "Handbook of Electrochemical constants". Since activity coefficients could not be obtained for sodium and potassium oleate solutions, it was not possible to calculate  $E_O$ 's and  $\bar{t}_+$  values for these systems.

Several attempts were made to calculate the value of the observed BIP's. The Lewis and Sargent potential has already been described and is equivalent to the liquid junction potential<sup>6</sup>.

The transport number  $E_O$  is identical to that developed by Sollner<sup>8</sup> and is

$$E_O = \frac{RT}{F} \ln \frac{\bar{t}_+}{\bar{t}'_+} \quad \text{where } \bar{t}_+ \text{ and } \bar{t}'_+ \text{ are the mobilities of the permeating ions.}$$

The Diffusion coefficient  $E_o$  is the general potential resulting from complete membrane diffusion control<sup>9,10</sup>.

$$E_o = \frac{RT}{F} \ln \frac{\bar{D}_A A'_A \lambda_B}{\bar{D}_B A''_B \lambda_A}$$

This expression holds for counter ions of equal valence. The  $\bar{D}$ 's are average diffusion coefficients and the  $\lambda$ 's are average values of the ion conductances.

None of the above formulations gave a BIP close to the observed BIP. The sum of the three values begins to approach the observed value but no theoretical significance can be attached to this.

Table 16 summarizes the permselective properties of nonpolymeric collodion - soap membranes. Table 17 summarizes the permselective properties of the early polysoap - collodion membranes which were made using prepackaged Baker and Fisher collodion solutions.

Despite the preponderant cation specificity of the PS 3-1-1-1 and PS 3-1-2-1 membranes, it is possible to demonstrate the generation of anion derived BIP's. This was done by using equimolar salt solutions having a cation in common but two different anions. Since  $\bar{t}^-$  is always finite (though sometimes small) a measurable BIP should be observed. No particular significance has yet been placed on the large absolute values of the anionic BIP's. The cation and anion membrane transference numbers for this particular membrane are given in Table 19 for various potassium halide concentration cells.

Pauling<sup>1</sup> suggested a remarkable theory to account for the loss of consciousness associated with general anesthesia. He postulated that the loss of consciousness induced by cooling of the brain is similar to that produced by a non-polar anesthetizing agent. The anesthetizing agent merely serves to raise the "freezing point" for the aqueous phase of the nerve membrane. In the presence of anesthetizing agents such

as chloroform and ether this "freezing point" may be raised to the level of normal body temperatures. The loss of consciousness under these conditions is presumably due to an increase in the impedance of the neural network and is associated with hydrate formation within the nerve membrane.

The effect of  $\text{CH}_3\text{Cl}$  on the  $\text{NaCl}/\text{KCl}$  BIP is shown in Figure 26. Note that the difference between the BIP's of the treated and untreated membrane become very great at low temperatures and almost superimpossible at higher temperatures. If an increasing impedance in the aqueous phase parallels a lower BIP, the potential should drop rapidly as a function of temperature in the case of the "anesthetized" membrane. It is generally conceded that in human subjects anesthesia is completely reversible. In the polysoap membrane system the effect is not completely reversible. The partially reversible character of this effect is shown in Figure 27. Repeated washing of the  $\text{CHCl}_3$  treated membrane raises the BIP to intermediate levels. Lack of 100% reversibility may be due to a solvent effect (i.e., some dissolution of the  $\text{CH}_3\text{Cl}$  soluble portion of the collodion-polysoap structure). Active membrane systems in a living cell may reverse this apparently "irreversible" effect.

At constant temperature the magnitude of the BIP decreases steadily with increasing  $\text{CH}_3\text{Cl}$  concentration (Figure 28). Attempts to "anesthetize" this membrane by treatment with nitrogen and argon at atmospheric pressures were inconclusive (Table 20). Polysoap cation exchange membranes offer several advantages over resin exchangers. Polysoaps of high molecular weight are insoluble in water, as are cross-linked exchangers. The polysoaps may be dissolved in solvent other than water and these solutions may be used to produce large sheets by large scale casting techniques. Polysoaps may be produced from inexpensive starting materials by a simple Friedel-Crafts alkylation.

Although Melpar has not yet synthesized any completely water insoluble polysoaps (of mol. wt. in excess of 100,000) it should be possible to do so. It is possible that these polysoaps could be used without a collodion supporting and retaining membranes.

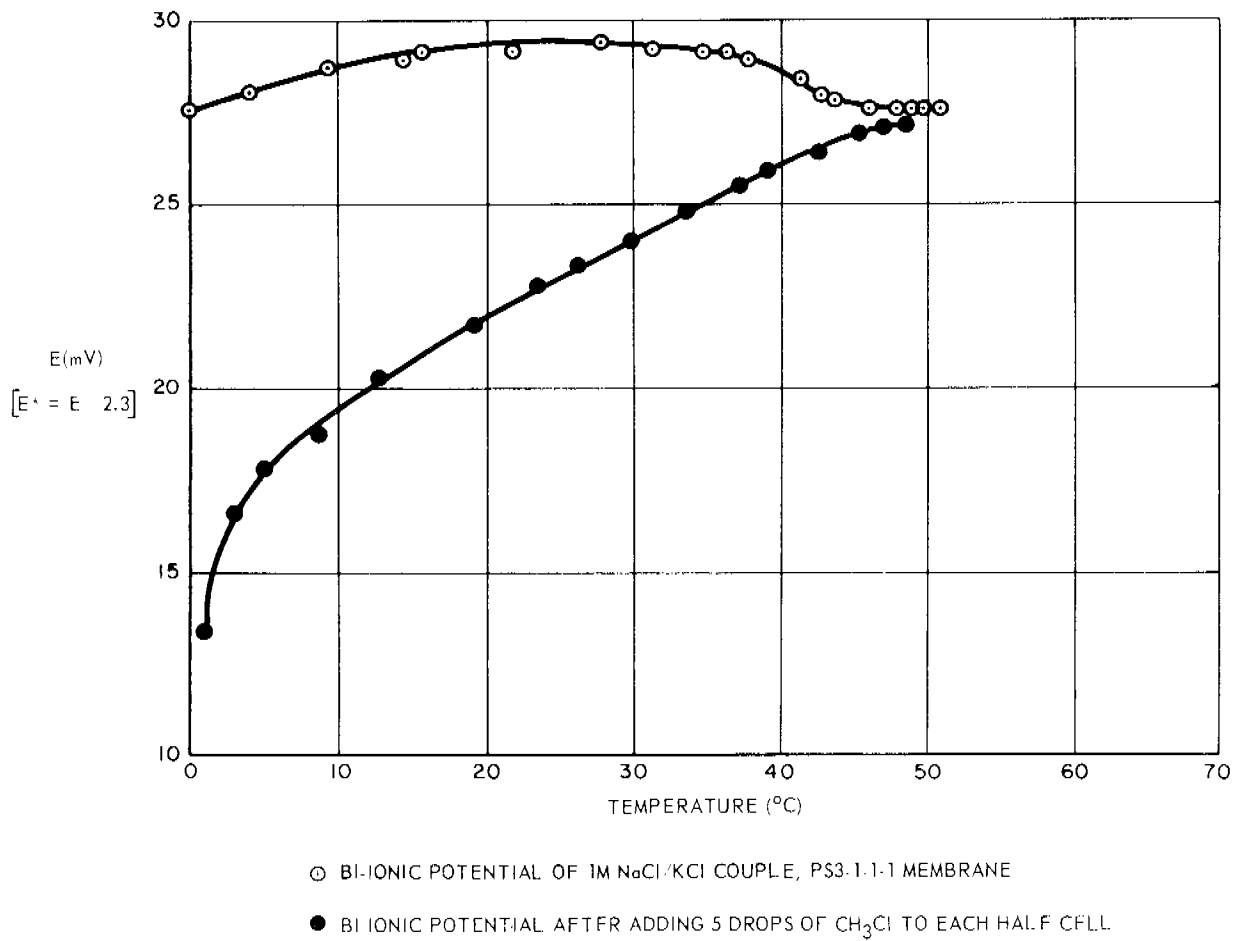


Figure 26. Temperature Dependence of BIP and Check of Pauling Hypothesis

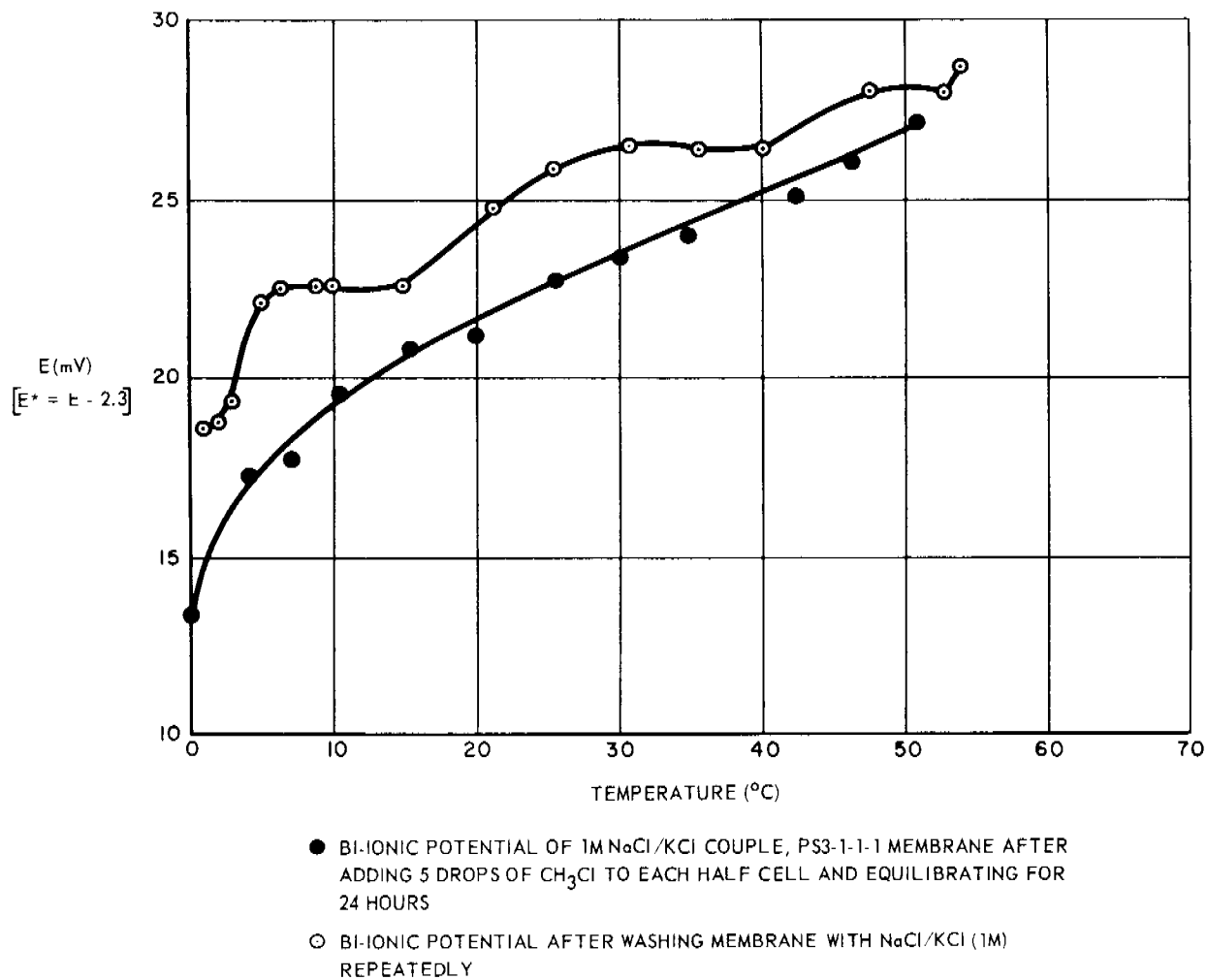


Figure 27. Temperature Dependence of BIP and Test of Reversibility of the Effect of  $\text{CH}_3\text{Cl}$

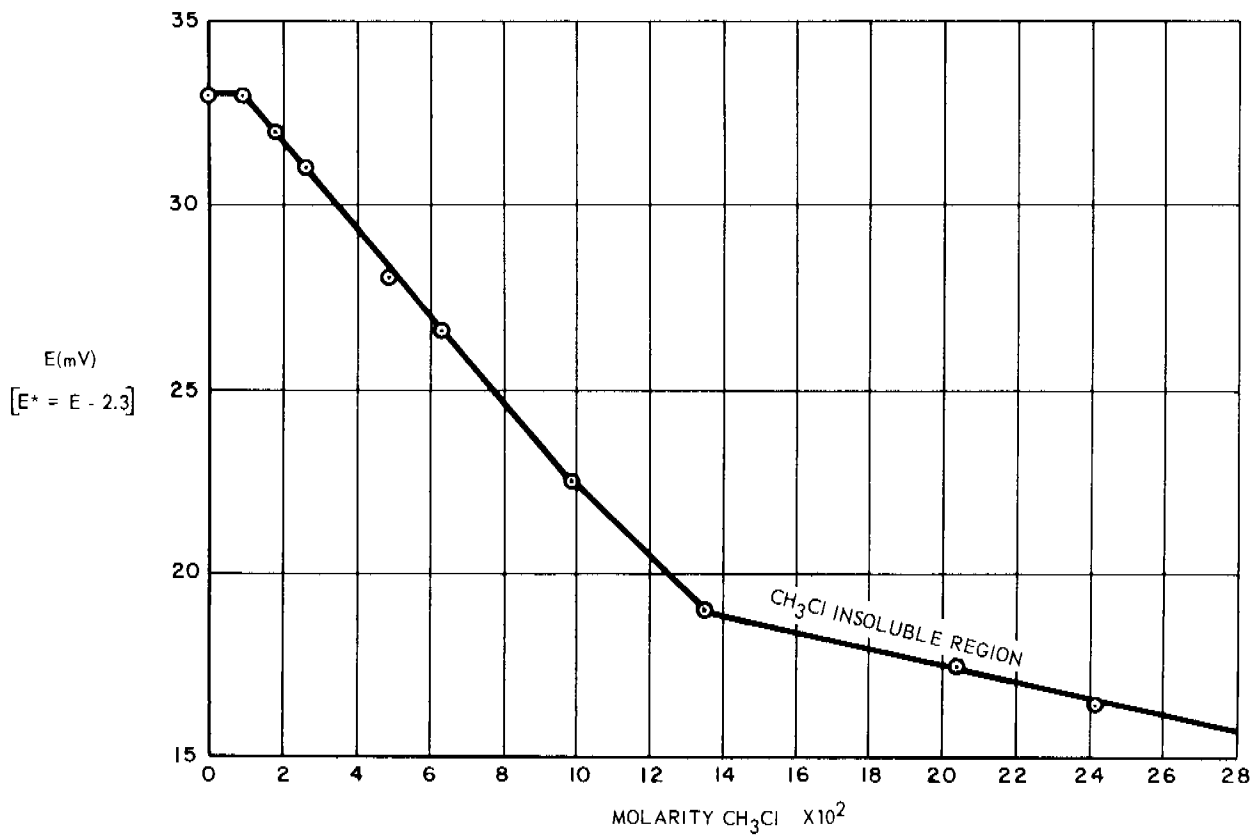


Figure 28. BIP vs. Concentration of  $\text{CH}_3\text{Cl}$  (PS 3-1-1-1 Membrane; 1 M NaCl/KCl couple,  $T = 1.4^\circ\text{C}$ )

A crude extrapolation was made to permit estimating the power output of a large cell employing a type PS 3-1-1-1 membrane used between brine and sea water electrolytes. The "sea water" was prepared by dissolving "Neptune Salts" in water in the ratio of 5 oz. to the gallon. "Brine" was simply a saturated solution of "Neptune Salts" at 25 degrees.

The brine - sea water concentration cell had an internal resistance of  $0.6 \times 10^6$  ohm. 0.1 uamp flowed through an external shunt under a difference of potential of 50 mV. Since the membrane area was 5.31 sq. cm., the power density was only 5 millimicrowatt.

Since the membrane may be considered to consist of a number of resistance elements in parallel, a larger sheet should exhibit a lower resistance. The resistance of a sheet one sq. meter in area should be

$$\frac{5.31 \text{ cm}^2}{10^6} \times 0.6 \times 10^6 = 0.32 \text{ ohm}$$

The current flowing through a shunt under these conditions should be

$$\frac{50 \text{ V}}{0.32} = 0.16 \text{ amp}$$

A number of these membranes could be placed in series, in the manner of construction of a voltaic pile. The individual membrane potentials and resistances would be additive. A cell occupying one cubic meter and containing 100 membranes in series should exhibit a total resistance of 32 ohms and a 50 volt potential. If the maximum current were only limited by the internal resistance of the cell (shunt in external circuit) the power output would be approximately 8 watts. These units could then be connected in parallel or series to produce the required output. With an improvement in membranes and a more sophisticated geometric arrangement, solar powered desalination plant might be supplied with power sufficient to operate pumping machinery and support systems. Utilization of the work potential of the brine-sea water couple could serve to lower the operating costs of other types of desalination plants.

## 5. CONCLUSIONS AND SUMMARY

These facts seem to indicate that both barium ions and bound water are somehow involved in the conductance transition which occurs when the multilayer membranes are heated. The rather low temperature at which the transition occurs strongly implicates the bound water as the principal cause of the effect. It must also be borne in mind that the choice of barium as the cation incorporated in the multilayer structure was not fortuitous. The original hypothesis which generated this experimental approach called for "order-disorder" transitions to occur in the polar sheets as the temperature was raised. In order for this to happen, the cation must be approximately the same size as oxygen. The oxygen could come from either the carboxyl groups of the acid or from the water. Barium fulfills this requirement, and is incidentally about the same size as potassium. Calcium, on the other hand, is considerably smaller than oxygen, and therefore would not permit a low energy "reshuffling" of associated atoms (cation and coordinated oxygen atoms) to a new, stable crystallographic state. Therefore, it appears that our results, although of a preliminary nature, are consistent with the original hypothesis.

The progress of the studies undertaken in the program up to this time indicate that although no gross structural alterations occurred in the synthetic ionic lipid single crystal, a process which has the appearance of a phase transition does seem to occur. Results pursued with emphasis on reproducing the results and establishing the limits of precision lead to another experimental approach.

Studies were made of the relationship between the permselective properties of a collodion supporting matrix and the total permselectivity of a collodion - polysoap - collodion laminate. Several methods were developed which permit control of the "pore size" of the collodion supporting structures. The "pore size" of the collodion could be controlled by the choice of proper solutes (e.g. glycerol) or swelling solvents (e.g. methanol). Soluble solid substances (e.g. oxalic acid or sucrose) could not be used because crystallization occurs as the solvent evaporates.

A study was made of the relationship between the magnitude of the BIP's (bi-ionic potentials), concentration cell potentials and salt diffusion rates through collodion membranes with respect to membrane preparation procedures and membrane thickness.

An attempt was made to study the effect of the solvent freezing point on the temperature dependence of the BIP. Dimethylformamide and dimethylsulfoxide were not adequate solvents of NaCl and KCl under water-free conditions. This approach to experimentally testing the Pauling hypothesis<sup>1</sup> was dropped in favor of the alternate method described in this report.

The Pauling theory of intra-membrane hydrate formation was tested by observing the effect of the anesthetizing agents, chloroform, nitrogen and argon on the temperature dependence of the BIP.

A rapid method was devised for the preparation of strong, delamination-resistant, highly permselective collodion-polysoap-collodion membranes. These membranes were studied as both cation and anion exchangers.

Several theories of the origin of the BIP<sup>11</sup> were used to obtain calculated values. These calculated values were much smaller than the corresponding observed BIP's in all instances.

An analysis was made of the practicality of using inexpensive polysoap cation exchange membranes to extract useful electrical power from the brine output of a desalination plant.

## 6. RECOMMENDATIONS FOR FUTURE WORK

In view of the fact that membrane (multilayer, soap, polysoap) transitions were observed below the respective Kraft points, future work should involve a thorough study of aqueous phase phenomena.

This study should be designed as an experimental test of the Pauling hypothesis involving clathrate formation in the aqueous phase of lipid-like membranes. The experimental approaches should involve:

1. Replacement of  $H_2O$  by  $D_2O$  in bi-ionic (and concentration) cell  $dV/dT$  studies.

2. A full investigation of the partially reversible "Pauling" effect, with particular emphasis on the effect of pressurized Xenon on  $dV/dT$  exhibited by bi-ionic and concentration cells.

3. An independent study of the formation of clathrate (soft-ice) structures at temperatures above the respective freezing points of  $H_2O$  and  $D_2O$ . A cooled NMR cell should be used to determine changes in proton band width of  $H_2O$  "soft-ice" forms. NMR could not be used on  $D_2O$  systems but could be an interesting "diluent" for stoichiometric NMR studies.

4. The Rudin Membrane<sup>12</sup> should be investigated with respect to points 1-3 since this is held to be the best available model of a natural biological membrane.

---

<sup>12</sup> Mueller, et. al., Circulation, 26, 1167 (1962)

7. REFERENCES

1. Pauling, L., *Science*, 134, 15 (1961).
2. Medalia, A. I., Freedman, H. H., Sinha, S., *J. of Polymer Sci.*, 40, 15 (1959).
3. Gregor and Schonhorn, *JACS*, 81, 3911 (1959).
4. Iangmuir and Schaefer, *JACS*, 58, 284 (1936).
5. Clarke, J. T., Marinsky, J. A., Juda, W., Rosenberg, N. W., Alexander, S., *J. Phys. Chem.*, 56, 100 (1952).
6. Lewis and Sargent, *J. Am. Chem. Soc.*, 31, 363 (1909).
7. Parsons, R., "Handbook of Electrochemical Constants", Butterworths Scientific Publications, London, 1959.
8. Sollner, K., *J. Phys. Chem.*, 53, 1211, 1226, (1949).
9. Helfferich, F., *Discussions Faraday Soc.*, 21, 83 (1956).
10. Helfferich, F., "Ion Exchange", McGraw-Hill Book Co., Inc., New York, New York, 1962.
11. Lakshiminarayanaiah, N., *Chem. Rev.*, 65, 491 (1965).